11

Fatigue Crack Growth

OBJECTIVES

- Apply the stress intensity factor K of fracture mechanics to fatigue crack growth and to environmental crack growth, and understand test methods and trends in behavior.
- Explore fatigue crack growth rate curves, da/dN versus ΔK, including fitting common equations and evaluating R-ratio (mean stress) effects.
- Calculate the life to grow a fatigue crack to failure, including cases requiring numerical integration and cases of variable amplitude loading. Employ such calculations to evaluate safety factors and inspection intervals.

11.1 INTRODUCTION

The presence of a crack can significantly reduce the strength of an engineering component due to brittle fracture, as already discussed in Chapter 8. However, it is unusual for a crack of dangerous size to exist initially, although this can occur, as when there is a large defect in the material used to make a component. In a more common situation, a small flaw that was initially present develops into a crack and then grows until it reaches the critical size for brittle fracture.

Crack growth can be caused by cyclic loading, a behavior called *fatigue crack growth*. However, if a hostile chemical environment is present, even a steady load can cause *environmental crack*

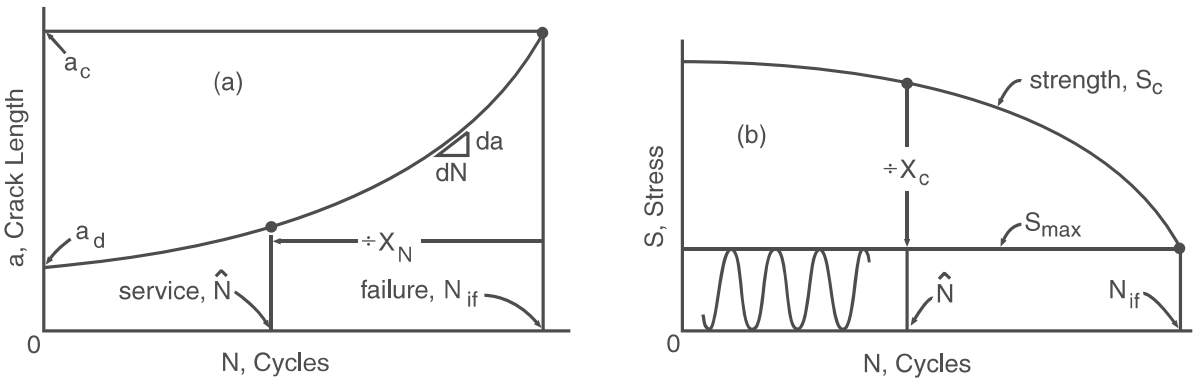

Figure 11.1 Growth of a worst-case crack from the minimum detectable length a_d to failure (a), and the resulting variation in worst-case strength (b).

growth. Both types of crack growth can occur if cyclic loads are applied in the presence of a hostile environment, especially if the cycling is slow or if there are periods of steady load interrupting the cycling. This chapter primarily considers fatigue crack growth, but limited discussion of environmental crack growth is included near the end in Section 11.10.

Engineering analysis of crack growth is often required and can be done with the stress intensity concept, K, of fracture mechanics. Recall from Chapter 8 that K quantifies the severity of a crack situation. Specifically, K depends on the combination of crack length, loading, and geometry given by

$$K = FS\sqrt{\pi a} \tag{11.1}$$

where a is crack length, S is nominal stress, and F is a dimensionless function of geometry and the relative crack length $\alpha = a/b$. The rate of fatigue crack growth is controlled by K. Hence, the dependence of K on a and F causes cracks to accelerate as they grow. The variation of crack length with cycles is thus similar to Fig. 11.1(a).

The analysis and prediction of fatigue crack growth has assumed major importance for large engineered items, especially where safety is paramount, as for large aircraft and for components in nuclear power plants. Note that the stress-based approach to fatigue of Chapters 9 and 10 does not consider cracks in a specific and detailed manner. Hence, this chapter provides an introduction to crack growth, including materials testing, trends in materials behavior, and prediction of the life to grow a crack to failure.

11.2 PRELIMINARY DISCUSSION

Before proceeding in detail, it is useful to describe the general nature of crack growth analysis and the need for it, and further to present some definitions.

11.2.1 Need for Crack Growth Analysis

It has been found from experience that careful inspection of certain types of hardware often reveals cracks. For example, this is the case for large welded components, such as pressure vessels and

bridge and ship structure, for metal structure in large aircraft, and for large forgings, as in the rotors of turbines and generators in power plants. Cracks are especially likely to be found in such hardware after some actual service usage has occurred. The possibility of cracks strongly suggests that specific analysis based on fracture mechanics is appropriate.

Let us assume that a certain structural component may contain cracks, but none are larger than a known *minimum detectable length* a_d. This situation could be the result of an inspection that is capable of finding all cracks larger than a_d, so that all such cracks have been repaired, or the parts scrapped. (Inspections for cracks are done by a variety of means, including visual examination, X-ray photography, reflection of ultrasonic waves, and application of electric currents, where in the latter case a crack causes a detectable disturbance in the resulting voltage field.) This worst-case crack of initial length a_d then grows until it reaches a critical length a_c, where brittle fracture occurs after N_{if} cycles of loading. If the number of cycles expected in actual service is $\hat{N}$, then the safety factor on life is

$$X_N = \frac{N_{if}}{\hat{N}} \tag{11.2}$$

This situation is illustrated in Fig. 11.1(a). Such a safety factor is needed because uncertainties exist as to the actual stress that will occur in service, the exact a_d that can be reliably found, and the crack growth rates in the material.

The critical strength for brittle fracture of the member is determined by the current crack length and the fracture toughness K_c for the material and thickness involved:

$$S_c = \frac{K_c}{F\sqrt{\pi a}} \tag{11.3}$$

As the worst-case crack grows, its length increases, causing the worst-case strength S_c to decrease, with failure occurring when S_c reaches $S_{\max}$, the maximum value for the cyclic loading applied in actual service. This is illustrated in Fig. 11.1(b). The safety factor on stress against sudden brittle fracture due to the applied cyclic load is

$$X_c = \frac{S_c}{S_{\max}} \tag{11.4}$$

Such a safety factor is generally needed in addition to X_N because of the possibility of an unexpected high load that exceeds the normal cyclic load. Within the expected actual service life, X_c decreases and has its minimum value at the end of this service life.

It sometimes occurs that the combination of minimum detectable crack length a_d and cyclic stress is such that the safety margin, as expressed by X_N and X_c, is insufficient. Predicted failure prior to reaching the actual service life, $X_N < 1$, may even be the case. *Periodic inspections* for cracks are then necessary, following which any cracks exceeding a_d are repaired, or the part replaced. This ensures that, after each inspection, no cracks larger than a_d exist. Assuming that inspections are done at intervals of N_p cycles, the length of the worst-case crack increases due to growth between inspections, varying as shown in Fig. 11.2. The safety factor on life is then

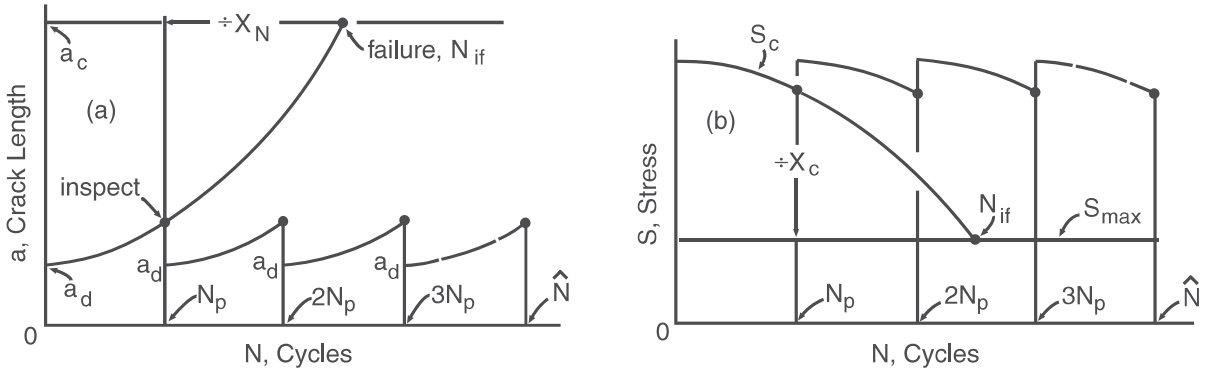

Figure 11.2 Variation of worst-case crack length (a), and strength (b), where periodic inspections are required.

determined by the inspection period:

$$X_N = \frac{N_{if}}{N_p} \tag{11.5}$$

After each inspection, the worst-case strength of the member temporarily increases, as shown in Fig. 11.2(b). The safety factor on stress is lowest just prior to each inspection.

Analysis based on fracture mechanics allows the variations in crack length and strength to be estimated so that safety factors can be evaluated. Where periodic inspections are necessary, fracture mechanics analysis thus permits a safe inspection interval to be set. For example, for large military and civilian aircraft, cracks are so commonly found during periodic inspections that safe operation and economic maintenance are both critically dependent on fracture mechanics analysis. The term *damage-tolerant design* is used to identify this approach of requiring that structures be able to survive even in the presence of growing cracks.

In reality, the detectable crack length a_d is not an absolute limit, as the probability of finding a crack in inspection increases with crack size, but is never 100%. For example, in the aircraft industry, values of a_d for various inspection methods are generally established as the size that can be found with 90% probability at a confidence level of 95%. On this basis, the better inspection methods give a_d values on the order of 1 or 2 mm under normal circumstances. Note that a_d is usually defined as the depth of a surface crack or half the width of an internal crack, on the basis of typical flaw geometries, as in Figs. 8.17 and 8.19. Cracks as small as $a = 0.1$ mm can be found, but a_d values this small can be justified only in special cases.

In addition to design applications, analysis of crack growth life is also useful in situations where an unexpected crack has been found in a component of a machine, vehicle, or structure. The remaining life can be calculated to determine whether the crack may be ignored, whether repair or replacement is needed immediately, or whether this can be postponed until a more convenient time. Situations of this sort have arisen in steel-mill machinery, where an immediate shutdown would disrupt operations and perhaps cause a large employee layoff. Similar situations have also occurred in turbine-generator units in major electrical power plants, where fracture of a large steel component could cause a power outage and expenditures of millions of dollars.

11.2.2 Definitions for Fatigue Crack Growth

Consider a growing crack that increases its length by an amount Δa due to the application of a number of cycles ΔN. The rate of growth with cycles can be characterized by the ratio $\Delta a/\Delta N$ or, for small intervals, by the derivative da/dN. A value of *fatigue crack growth rate*, da/dN, is the slope at a point on an a versus N curve, as in Fig. 11.1(a).

Assume that the applied loading is cyclic, with constant values of the loads $P_{\max}$ and $P_{\min}$. The corresponding gross section nominal stresses $S_{\max}$ and $S_{\min}$ are then also constant. For fatigue crack growth work, it is conventional to use the stress range ΔS and the stress ratio R, which are defined as in Eqs. 9.1 and 9.3:

$$\Delta S = S_{\max} - S_{\min}, \qquad R = \frac{S_{\min}}{S_{\max}} \tag{11.6}$$

The primary variable affecting the growth rate of a crack is the range of the stress intensity factor. This is calculated from the stress range ΔS:

$$\Delta K = F\ \Delta S\sqrt{\pi a} \tag{11.7}$$

The value of F depends only on the geometry and the relative crack length, $\alpha = a/b$, just as if the loading were not cyclic. Since, according to Eq. 11.1, K and S are proportional for a given crack length, the maximum, minimum, range, and R-ratio for K during a loading cycle are respectively given by

$$\begin{aligned} K_{\max} &= F S_{\max}\sqrt{\pi a}, \qquad & K_{\min} &= F S_{\min}\sqrt{\pi a} \\ \Delta K &= K_{\max} - K_{\min}, \qquad & R &= \frac{K_{\min}}{K_{\max}} \end{aligned} \tag{11.8}$$

Also, it may be convenient, especially for laboratory test specimens, to use the alternative expression of K in terms of applied force P, as discussed in Chapter 8 relative to Eq. 8.13:

$$\Delta K = F_P \frac{\Delta P}{t\sqrt{b}}, \qquad R = \frac{P_{\min}}{P_{\max}} \tag{11.9}$$

11.2.3 Describing Fatigue Crack Growth Behavior of Materials

For a given material and set of test conditions, the crack growth behavior can be described by the relationship between cyclic crack growth rate da/dN and stress intensity range ΔK. Test data and a fitted curve for one material are shown on a log–log plot in Fig. 11.3. At intermediate values of ΔK, there is often a straight line on the log–log plot, as in this case. A relationship representing this line is

$$\frac{da}{dN} = C(\Delta K)^m \tag{11.10}$$

where C is a constant and m is the slope on the log–log plot, assuming, of course, that the decades on both log scales are the same length. This equation is identified with Paul Paris, who first used

it and who was influential in the first application of fracture mechanics to fatigue in the early 1960s.

At low growth rates, the curve generally becomes steep and appears to approach a vertical asymptote denoted ΔK_{th}, which is called the *fatigue crack growth threshold*. This quantity is interpreted as a lower limiting value of ΔK below which crack growth does not ordinarily occur. At high growth rates, the curve may again become steep, due to rapid unstable crack growth just

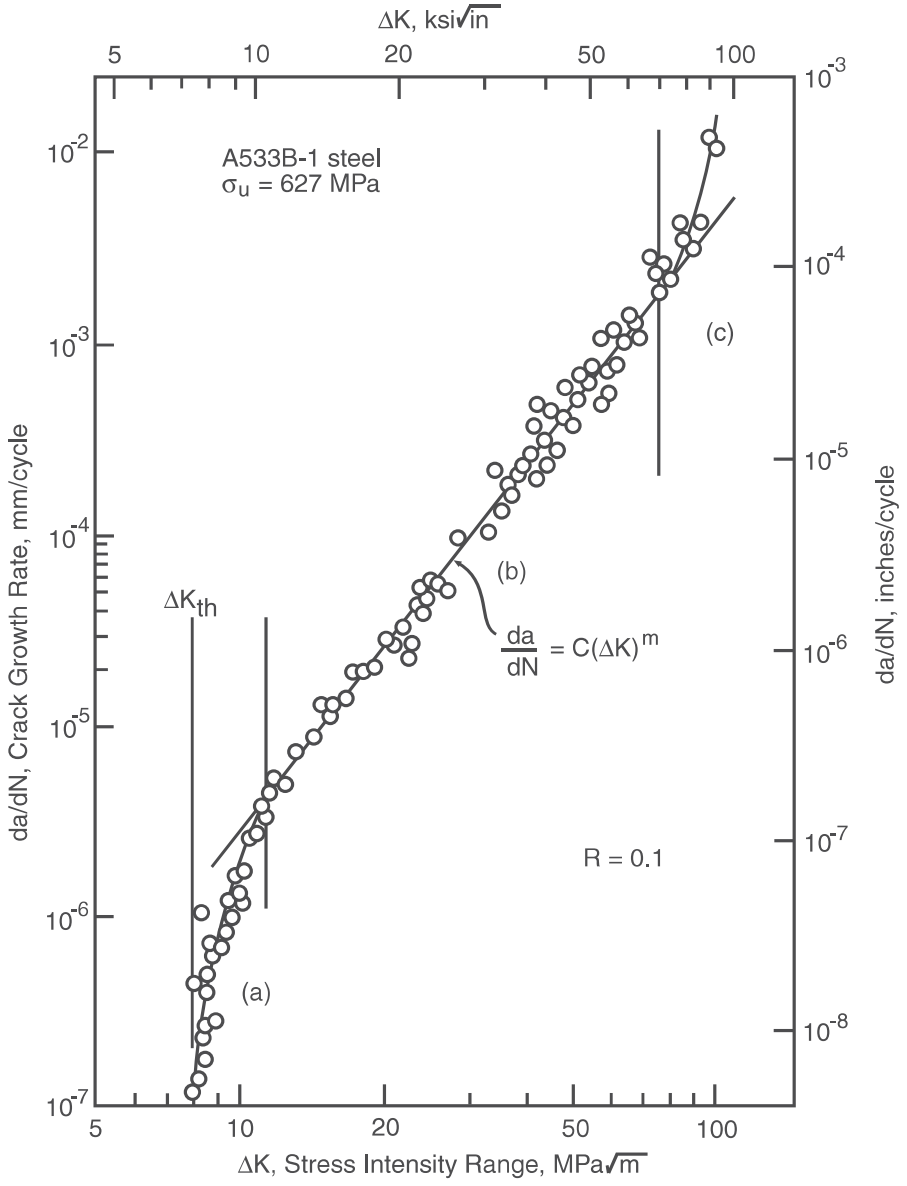

Figure 11.3 Fatigue crack growth rates over a wide range of stress intensities for a ductile pressure vessel steel. Three regions of behavior are indicated: (a) slow growth near the threshold ΔK_{th}, (b) intermediate region following a power equation, and (c) unstable rapid growth. (Plotted from the original data for the study of [Paris 72].)

prior to final failure of the test specimen. Such behavior can occur where the plastic zone is small, in which case the curve approaches an asymptote corresponding to $K_{\max} = K_c$, the fracture toughness for the material and thickness of interest. Rapid unstable growth at high ΔK sometimes involves fully plastic yielding. In such cases, the use of ΔK for this portion of the curve is improper, as the theoretical limitations of the K concept are exceeded.

The value of the stress ratio R affects the growth rate in a manner analogous to the effects observed in S-N curves for different values of R or mean stress. For a given ΔK, increasing R increases the growth rate, and vice versa. Some data illustrating this effect for a steel are shown in Fig. 11.4.

Constants C and m for the intermediate region where Eq. 11.10 applies have been suggested by Barsom (1999) for various classes of steel. These apply for $R \approx 0$ and are given in Table 11.1.

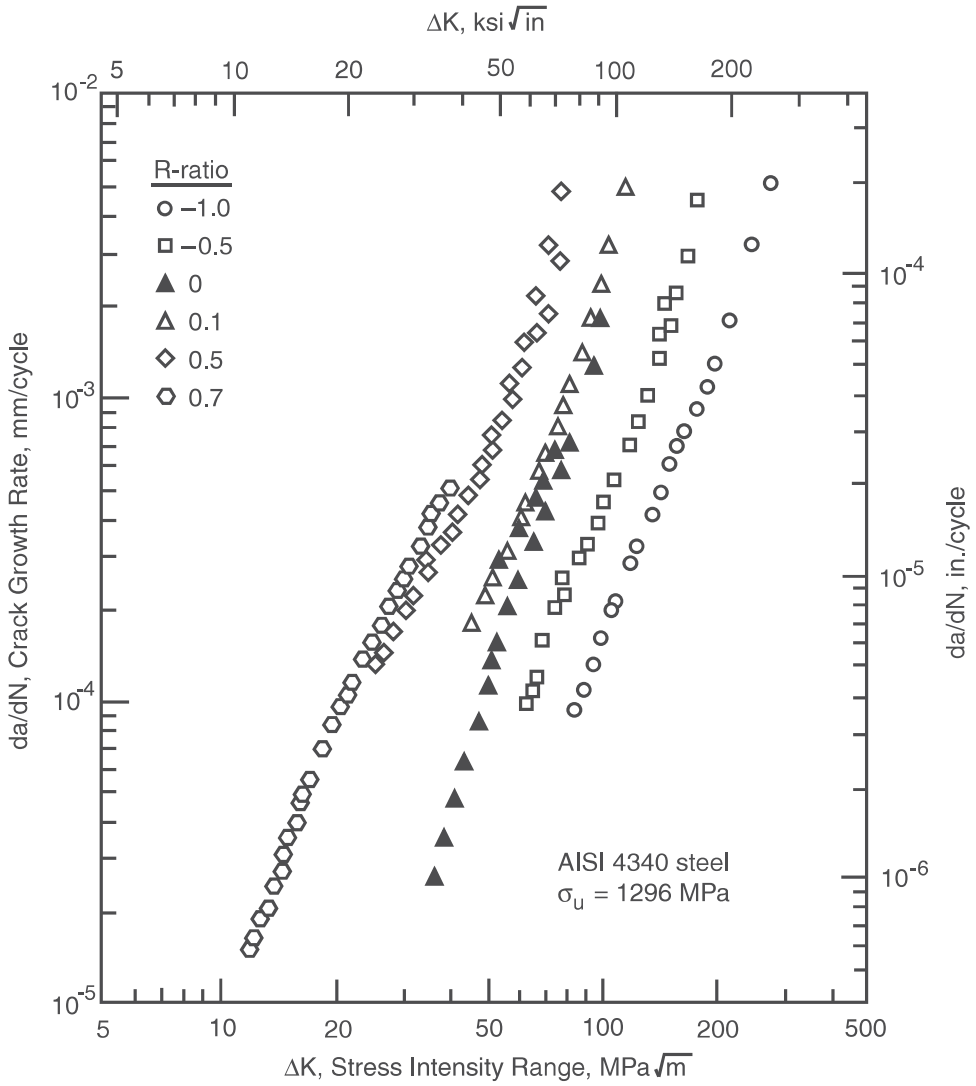

Figure 11.4 Effect of R-ratio on crack growth rates for an alloy steel. For $R < 0$, the compressive portion of the load cycle is here included in calculating ΔK. (Data from [Dennis 86].)

Table 11.1 Constants from Barsom (1999) for Worst-Case da/dN Versus ΔK Curves for Various Classes of Steel for $R \approx 0$

	Constants for $da/dN = C(\Delta K)^m$		
Class of Steel	C, $\frac{\text{mm/cycle}}{(\text{MPa}\sqrt{\text{m}})^m}$	C, $\frac{\text{in/cycle}}{(\text{ksi}\sqrt{\text{in}})^m}$	m
Ferritic-pearlitic	6.89×10^{-9}	3.6×10^{-10}	3.0
Martensitic	1.36×10^{-7}	6.6×10^{-9}	2.25
Austenitic	5.61×10^{-9}	3.0×10^{-10}	3.25

Note: For use with the Walker equation for $R > 0.2$, it is suggested that the given constants be employed as C_0 and m along with an approximate value of $\gamma = 0.5$.

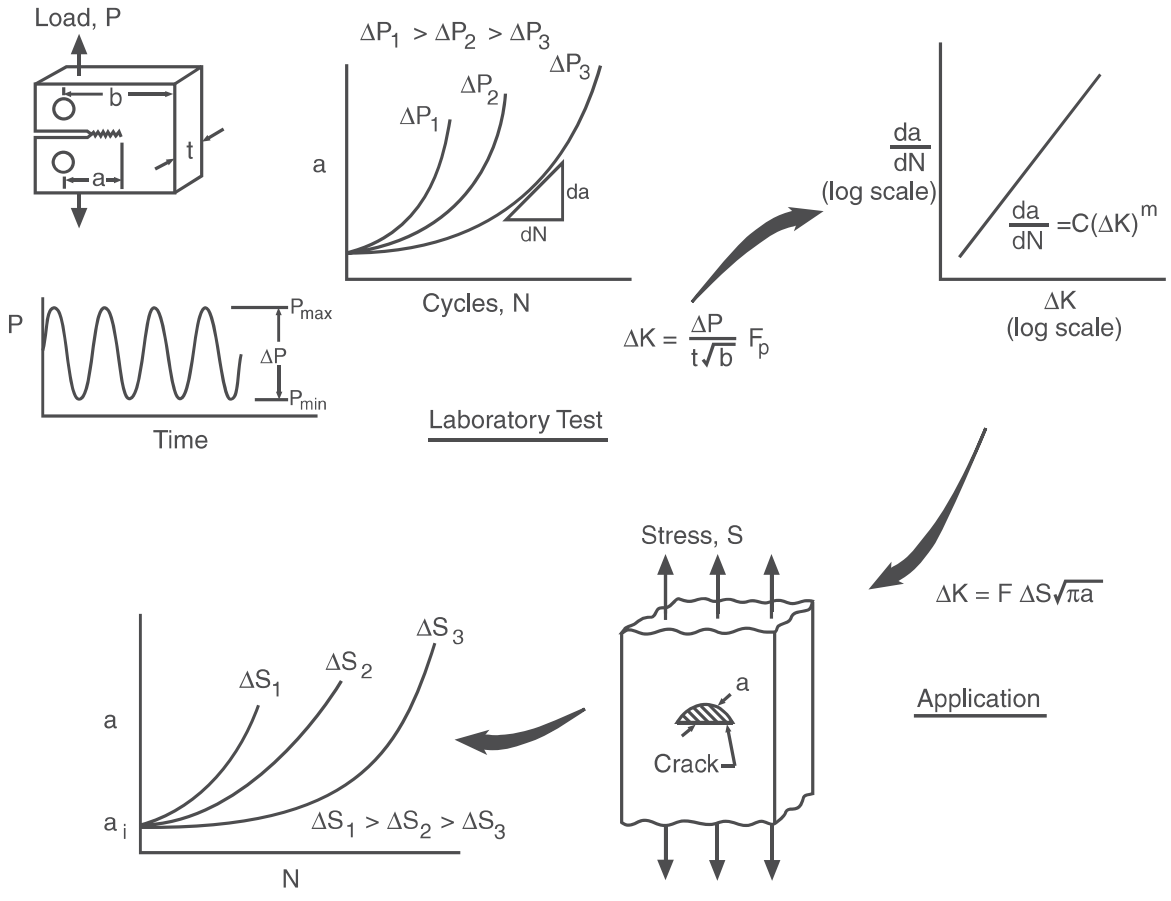

Figure 11.5 Steps in obtaining da/dN versus ΔK data and using it for an engineering application. (Adapted from [Clark 71]; used with permission.)

The value of m is important, as it indicates the degree of sensitivity of the growth rate to stress. For example, if $m = 3$, doubling the stress range ΔS doubles the stress intensity range ΔK, thus increasing the growth rate by a factor of $2^m = 8$.

11.2.4 Discussion

The logical path involved in evaluating the crack growth behavior of a material and using the information is summarized in Fig. 11.5. First, a convenient test specimen geometry is employed in tests at each of several different load levels, so that a wide range of fatigue crack growth rates is obtained. Growth rates are then evaluated and plotted versus ΔK to obtain the da/dN versus ΔK curve. This curve can be used later in an engineering application, with ΔK values being calculated as appropriate for the particular component geometry of interest. Crack length versus cycles curves for a specific initial crack length can then be predicted for the component, leading to life estimates and the determination of safety factors and inspection intervals as discussed earlier.

Example 11.1

Obtain approximate values of constants C and m, and give Eq. 11.10 for the data at $R = 0.1$ in Fig. 11.4.

Solution These data appear to fall along a straight line on this log–log plot, so it is reasonable to apply Eq. 11.10. Aligning a straight edge with the data gives a line that passes near two points as follows:

$$\left(\Delta K, \frac{da}{dN}\right) = \left(21, 10^{-5}\right) \qquad \text{and} \qquad \left(155, 10^{-2}\right)$$

Here, units of MPa$\sqrt{\text{m}}$ and mm/cycle are used. Now apply Eq. 11.10 to these two points, denoting them as $(\Delta K_A, da/dN_A)$ and $(\Delta K_B, da/dN_B)$:

$$da/dN_A = C(\Delta K_A)^m, \qquad da/dN_B = C(\Delta K_B)^m$$

Eliminate C between these two equations by dividing one into the other:

$$\frac{da/dN_A}{da/dN_B} = \left(\frac{\Delta K_A}{\Delta K_B}\right)^m$$

Taking logarithms of both sides and solving for m then gives

$$m = \frac{\log\left(da/dN_A\right) - \log\left(da/dN_B\right)}{\log\left(\Delta K_A\right) - \log\left(\Delta K_B\right)} = \frac{\log 10^{-5} - \log 10^{-2}}{\log 21 - \log 155} = 3.456$$

Next, obtain C by substituting this m and either known point into Eq. 11.10:

$$10^{-5}\frac{\text{mm}}{\text{cycle}} = C(21\ \text{MPa}\sqrt{\text{m}})^{3.456}, \qquad C = 2.696 \times 10^{-10}\frac{\text{mm/cycle}}{(\text{MPa}\sqrt{\text{m}})^m}$$

Note that C has the unusual units indicated that involve the exponent m. Hence, the desired relationship, with constants rounded to three significant figures, is

$$\frac{da}{dN} = 2.70 \times 10^{-10}(\Delta K)^{3.46} \qquad (\text{mm/cycle, MPa}\sqrt{\text{m}}) \qquad \textbf{Ans.}$$

Discussion If a more accurate fit is desired, the original source of the data should be consulted for numerical values of the data points and a log–log least squares line of the form $y = mx + b$ obtained. Taking logarithms of both sides of Eq. 11.10 then gives

$$\log \frac{da}{dN} = m \log (\Delta K) + \log C$$

$$y = \log \frac{da}{dN}, \qquad x = \log (\Delta K), \qquad m = m, \qquad b = \log C$$

11.3 FATIGUE CRACK GROWTH RATE TESTING

Standard methods for conducting fatigue crack growth tests have been developed, notably ASTM Standard No. E647. Two commonly used test specimen geometries are the standard compact specimen, Fig 8.16, and center-cracked plates, Fig. 8.12(a).

11.3.1 Test Methods and Data Analysis

In a typical test, constant amplitude cyclic loading is applied to a specimen of a size such that its width dimension b (as defined in Chapter 8) is perhaps 50 mm. Before starting the test, a precrack is necessary. This is accomplished by first machining a sharp notch into the specimen and then starting a crack by cyclic loading at a low level. Cyclic loading is then applied at the higher level to be used for the remainder of the test. The progress of the crack is recorded in terms of the numbers of cycles required for its length to reach each of 10 to 20 or more different values, with these being on the order of 1 mm apart for a specimen of size $b \approx 50$ mm. The resulting crack length data may then be plotted as discrete points versus the corresponding cycle numbers, as in Fig. 11.6.

To measure these crack lengths, one approach is simply to note by visual observation, through a low-power (20 to 50X) microscope, when the crack reaches various lengths that have been previously marked on the specimen. An arrangement for such a test is shown in Fig. 11.7. More sophisticated means may be used to measure crack lengths. For example, as the crack grows, the deflection of the specimen increases, resulting in decreased stiffness. This stiffness change may be measured and used to calculate the crack length. Another approach is to pass an electric current through the specimen and measure changes in the voltage field due to growth of the crack, from which we can obtain its length. Ultrasonic waves can also be reflected from the crack and used to measure its progress.

To obtain growth rates from crack length versus cycles data, a simple and generally suitable approach is to calculate straight-line slopes between the data points, as shown in Fig. 11.6.

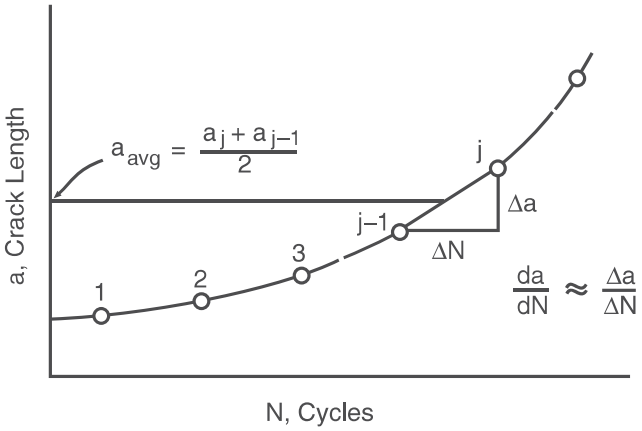

Figure 11.6 Crack growth rates obtained from adjacent pairs of *a* versus *N* data points.

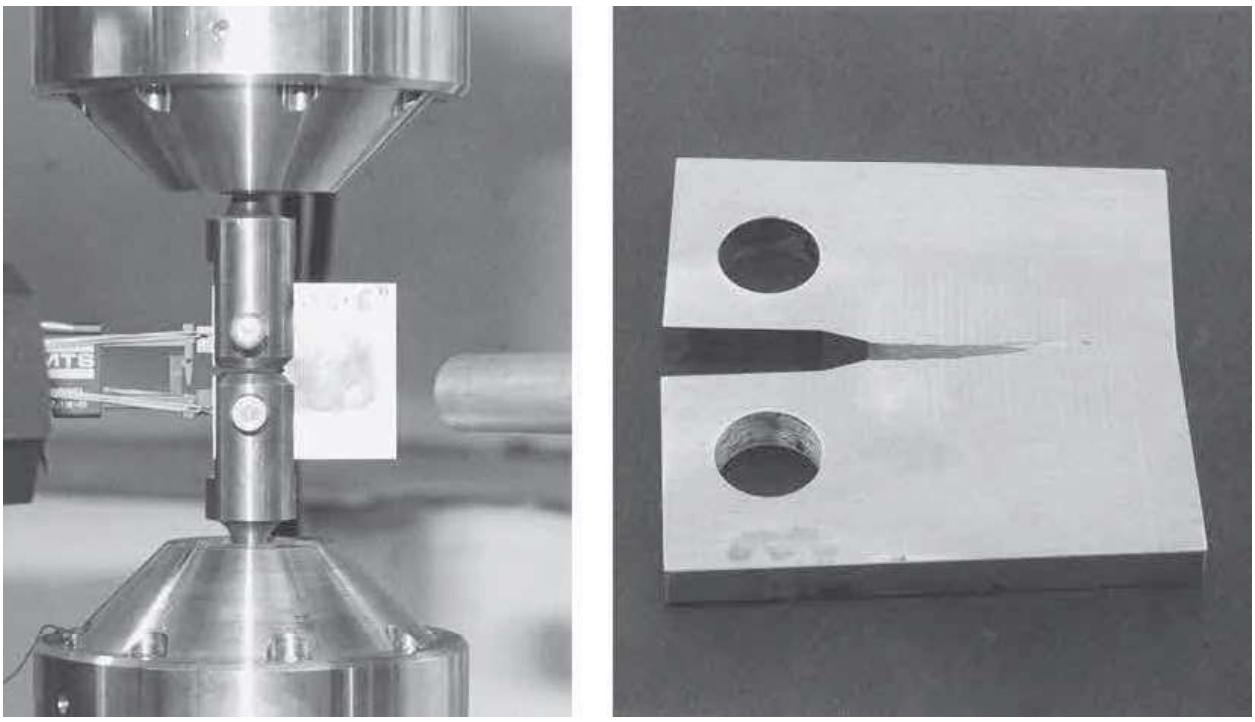

Figure 11.7 Crack growth rate test under way (left) on a compact specimen ($b = 51$ mm), with a microscope and a strobe light used to visually monitor crack growth. Cycle numbers are recorded when the crack reaches each of a number of scribe lines (right). (Photos by R. A. Simonds.)

If the data points are numbered $1, 2, 3 \ldots j$, then the growth rate for the segment ending at point number j is

$$\left(\frac{da}{dN}\right)_j \approx \left(\frac{\Delta a}{\Delta N}\right)_j = \frac{a_j - a_{j-1}}{N_j - N_{j-1}} \tag{11.11}$$

The corresponding ΔK is calculated from the average crack length during the interval with either of the two equations

$$\Delta K_j = F\ \Delta S\sqrt{\pi a_{\text{avg}}}, \qquad \Delta K_j = F_P \frac{\Delta P}{t\sqrt{b}} \tag{11.12}$$

whichever is more convenient. In the first equation,

$$a_{\text{avg}} = \frac{a_j + a_{j-1}}{2} \tag{11.13}$$

The geometry factor $F = F(\alpha)$ or $F_P = F_P(\alpha)$, where $\alpha = a/b$, is evaluated at the same average crack length, using

$$\alpha_{\text{avg}} = \frac{a_{\text{avg}}}{b} = \frac{a_j + a_{j-1}}{2b} \tag{11.14}$$

The foregoing procedure is valid only if the crack length is measured at fairly short intervals. Otherwise, the growth rate and K may differ so much between adjacent observations that the averaging involved causes difficulties. Detailed requirements are given in the ASTM Standard. Also, curve-fitting methods of evaluating da/dN, which are more sophisticated than simple point-to-point slopes, are sometimes used to smooth the scatter in the a versus N data. Fitting a polynomial over all of the data from a test usually does not work very well, but such a fit applied in an incremental manner to portions of the data works well, as described in the ASTM Standard.

Example 11.2

Crack length versus cycles data are given in Table E11.2(a) from a test on a center-cracked plate of 7075-T6 aluminum. The specimen had dimensions, as defined in Fig. 8.12(a), of $h = 445$, $b = 152.4$, and $t = 2.29$ mm. The force was cycled between zero and a maximum value of $P_{\max} = 48.1$ kN. Obtain da/dN and ΔK values from these data.

Solution The average growth rate between points 1 and 2 is obtained by applying Eq. 11.11 with $j = 2$:

$$\left(\frac{da}{dN}\right)_2 = \frac{a_2 - a_1}{N_2 - N_1} = \frac{7.62 - 5.08}{18{,}300 - 0} = 1.388 \times 10^{-4}\ \text{mm/cycle} \qquad \textbf{Ans.}$$

The corresponding ΔK is evaluated by using the average crack length from Eqs. 11.13 and 11.14 with $j = 2$:

$$a_{\text{avg}} = \frac{a_2 + a_1}{2} = \frac{7.62 + 5.08}{2} = 6.35\ \text{mm}, \qquad \alpha_{\text{avg}} = \frac{a_{\text{avg}}}{b} = \frac{6.35\ \text{mm}}{152.4\ \text{mm}} = 0.0417$$

To evaluate F for this geometry, Fig. 8.12(a) is employed. The value corresponding to α_{avg} is

$$F = \frac{1 - 0.5\alpha + 0.326\alpha^2}{\sqrt{1 - \alpha}} = \frac{1 - 0.5(0.0417) + 0.326(0.0417)^2}{\sqrt{1 - 0.0417}} = 1.001$$

Table E11.2

(a) Given Data			(b) Calculated Values				
j	a mm	N cycles	da/dN mm/cycle	a_{avg} mm	α_{avg}	F	ΔK MPa$\sqrt{\text{m}}$
1	5.08	0	—	—	—	—	—
2	7.62	18 300	1.39×10^{-4}	6.35	0.0417	1.001	9.74
3	10.16	28 300	2.54×10^{-4}	8.89	0.0583	1.002	11.53
4	12.70	35 000	3.79×10^{-4}	11.43	0.0750	1.003	13.09
5	15.24	40 000	5.08×10^{-4}	13.97	0.0917	1.004	14.49
6	17.78	43 000	8.47×10^{-4}	16.51	0.1083	1.006	15.78
7	20.32	47 000	6.35×10^{-4}	19.05	0.1250	1.008	16.99
8	22.86	50 000	8.47×10^{-4}	21.59	0.1417	1.010	18.13
9	25.40	52 000	1.27×10^{-3}	24.13	0.1583	1.013	19.21
10	30.48	57 000	1.02×10^{-3}	27.94	0.1833	1.017	20.77
11	35.56	59 000	2.54×10^{-3}	33.02	0.2167	1.025	22.74
12	40.64	61 000	2.54×10^{-3}	38.10	0.2500	1.034	24.65
13	45.72	62 000	5.08×10^{-3}	43.18	0.2833	1.045	26.52

Source: Data in [Hudson 69].

Hence, using $\Delta S = \Delta P/(2bt)$ in Eq. 11.12, we have

$$(\Delta K)_2 = F\ \Delta S\sqrt{\pi a_{avg}}$$

$$(\Delta K)_2 = 1.001\frac{48{,}100\,\text{N}}{2(152.4\,\text{mm})(2.29\,\text{mm})}\sqrt{\pi(0.00635\,\text{m})} = 9.74\,\text{MPa}\sqrt{\text{m}} \qquad \textbf{Ans.}$$

Similarly applying Eqs. 11.11 to 11.14 with $j = 3$, and then with $j = 4$, etc., gives the additional values seen in Table E11.2(b).

11.3.2 Test Variables

Crack growth tests are most commonly conducted under zero-to-tension loading, $R = 0$, or tension-to-tension loading with a small R value, such as $R = 0.1$. Variations of R in the range 0 to 0.2 have little effect on most materials, and tests in this range are accepted by convention as the standard basis for comparing the effects of various materials, environments, etc. It is usually necessary to test several specimens at different load levels to obtain data over a wide range of growth rates. Such results for a steel are shown in Figs. 11.8 and 11.9. For more complete data, groups of several tests at each of several R values can be conducted. Also, if data are desired in the ΔK_{th} region, a special decreasing load test is needed, as described in ASTM Standard No. E647.

A wide range of variables may affect fatigue crack growth rates in a given material, so that test conditions may be selected to include situations that resemble the anticipated service use of the material. Some of these variables are temperature, frequency of the cyclic load, and hostile chemical environments. Minor variations in the processing or composition of materials may affect fatigue crack growth rates due to the different microstructures that result. Hence, tests on different

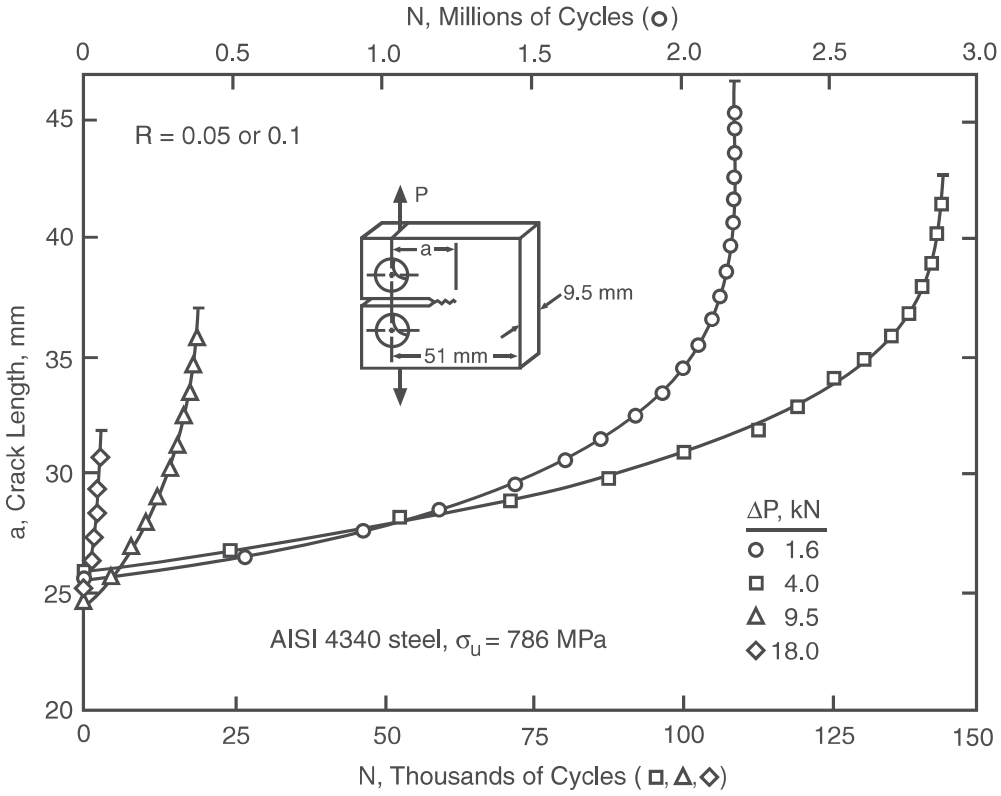

Figure 11.8 Crack length versus cycles data for four different levels of cyclic load applied to compact specimens of an alloy steel.

variations of a material may be conducted to aid in developing materials that can best resist fatigue crack growth.

11.3.3 Geometry Independence of *da*/*dN* versus ΔK Curves

For a given material and set of test conditions, such as a particular R value, test frequency, and environment, the growth rates should depend only on ΔK. This arises simply from the fact that K characterizes the severity of a combination of loading, geometry, and crack length, and ΔK serves the same function for cyclic loading. Hence, regardless of the load level, crack length, and specimen geometry, all da/dN versus ΔK data for a given set of test conditions should fall together along a single curve, except that some statistical scatter is, of course, expected. This occurs for the different load levels and crack lengths involved in Figs. 11.8 and 11.9. There should be a single trend even if more than one specimen geometry is included in the tests. Some data demonstrating geometry independence are shown in Fig. 11.10.

Such uniqueness of the da/dN versus ΔK curve for different geometries is a crucial test of the applicability of the K concept to both materials testing and engineering applications. (Recall Fig. 11.5.) This uniqueness has been sufficiently verified, so it is not generally necessary to include more than one test specimen geometry in obtaining materials data. However, difficulty with the applicability of ΔK can occur if there is excessive yielding, or for very small cracks, as discussed in Section 11.9 near the end of this chapter.

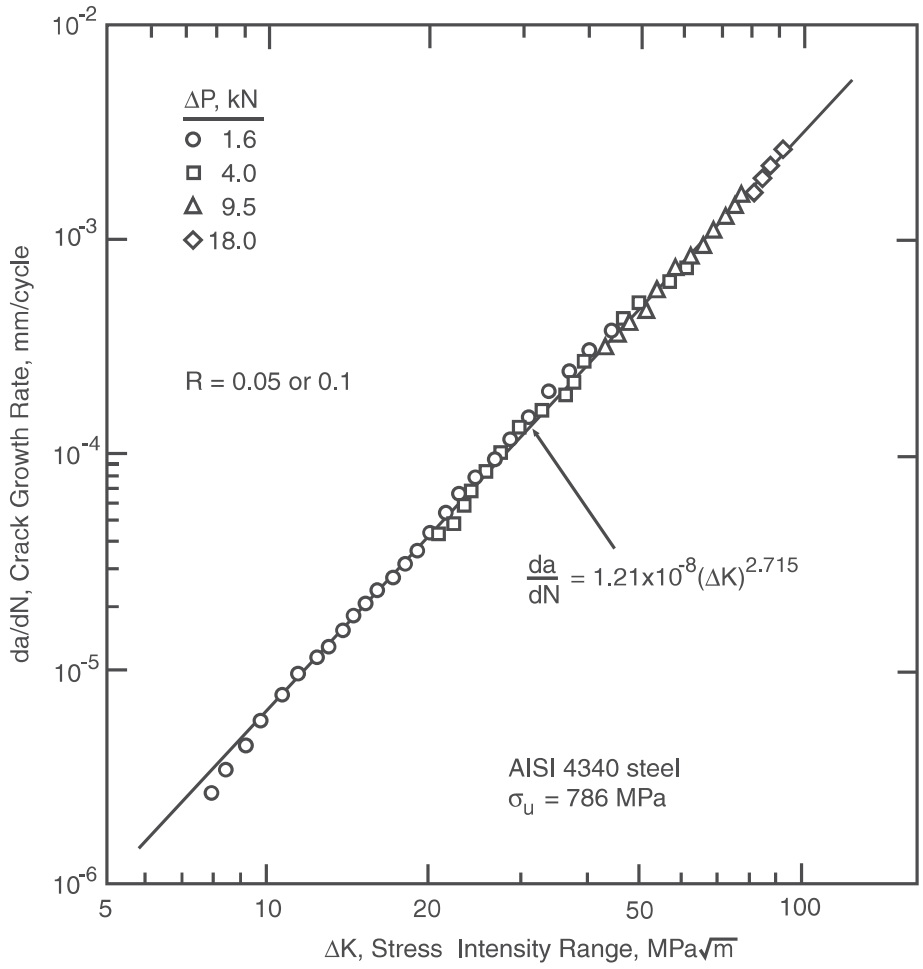

Figure 11.9 Data and least-squares fitted line for da/dN versus ΔK from the a versus N data of Fig. 11.8.

11.4 EFFECTS OF $R = S_{min}/S_{max}$ ON FATIGUE CRACK GROWTH

An increase in the R-ratio of the cyclic loading causes growth rates for a given ΔK to be larger, which has already been illustrated by Fig. 11.4. The effect is usually more pronounced for more brittle materials. For example, the granite rock of Fig. 11.11 shows an extreme effect, being sensitive to increasing R from 0.1 to only 0.2. In contrast, mild steel and other relatively low-strength, highly ductile, structural metals exhibit only a weak R effect in the intermediate growth rate region of the da/dN versus ΔK curve.

11.4.1 The Walker Equation

Various empirical relationships are employed for characterizing the effect of R on da/dN versus ΔK curves. One of the most widely used equations is based on applying the Walker relationship,

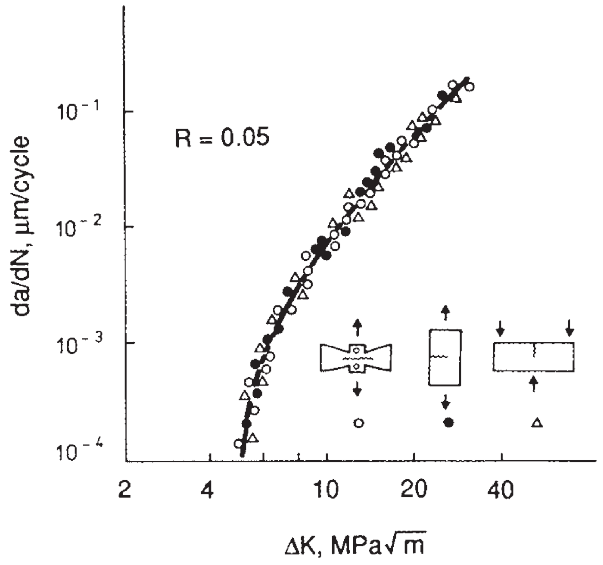

Figure 11.10 Fatigue crack growth rate data for a 0.65% carbon steel, demonstrating geometry independence. (Adapted from [Klesnil 80] p. 111; used with permission.)

Eq. 10.38, to the stress intensity factor K:

$$\overline{\Delta K} = K_{max}(1 - R)^{\gamma} \tag{11.15}$$

Here, γ is a constant for the material and $\overline{\Delta K}$ is an equivalent zero-to-tension ($R = 0$) stress intensity that causes the same growth rate as the actual K_{max}, R combination. By applying Eq. 9.4(a) to K, which gives $\Delta K = K_{max}(1 - R)$, Eq. 11.15 is seen to be equivalent to

$$\overline{\Delta K} = \frac{\Delta K}{(1 - R)^{1-\gamma}} \tag{11.16}$$

Let the constant C in Eq. 11.10 be denoted C_0 for the special case of $R = 0$.

$$\frac{da}{dN} = C_0 (\Delta K)^m \qquad (R = 0) \tag{11.17}$$

Since $\overline{\Delta K}$ is an equivalent ΔK for $R = 0$, we can substitute $\overline{\Delta K}$ for ΔK in Eq. 11.17:

$$\frac{da}{dN} = C_0 \left[\frac{\Delta K}{(1 - R)^{1-\gamma}} \right]^m \tag{11.18}$$

This represents a family of da/dN versus ΔK curves, which, on a log–log plot, are all parallel straight lines of slope m. Some manipulation gives

$$\frac{da}{dN} = \frac{C_0}{(1 - R)^{m(1-\gamma)}} (\Delta K)^m \tag{11.19}$$

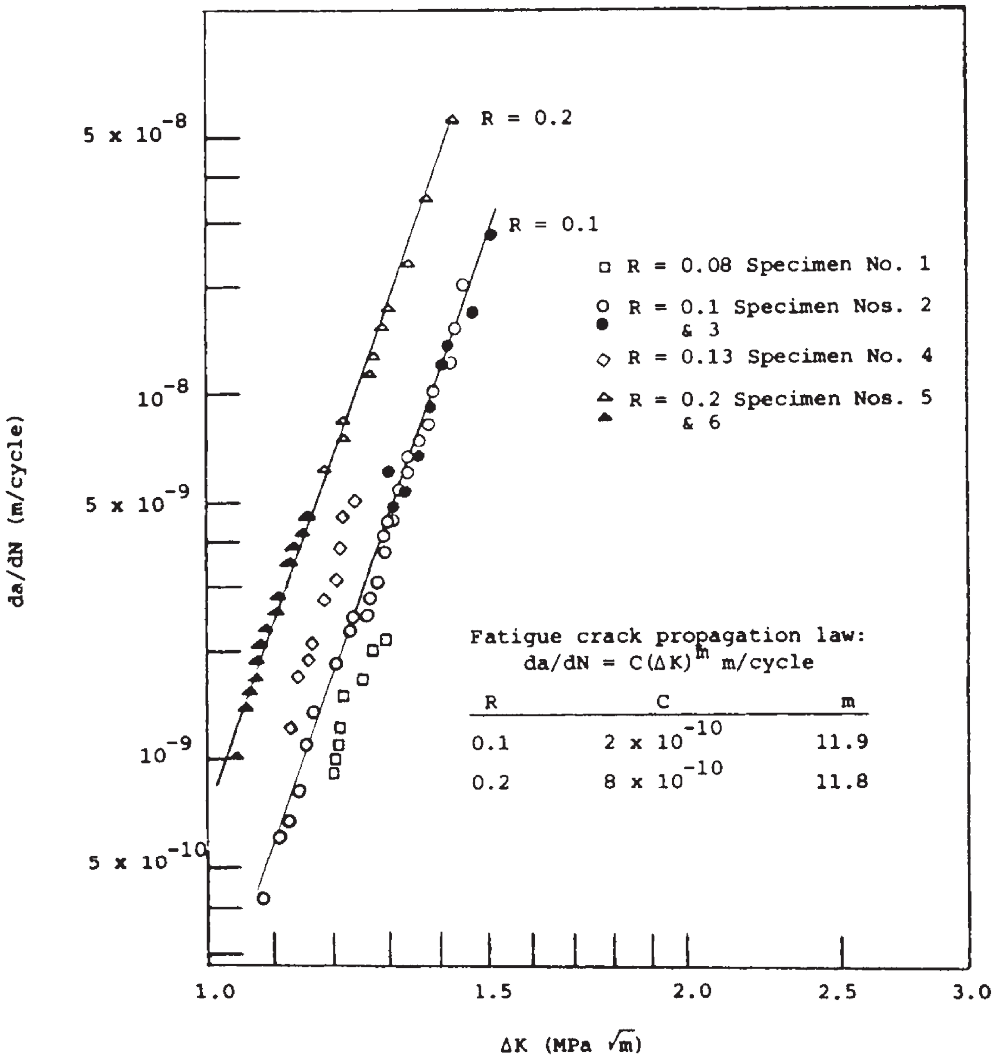

Figure 11.11 Effect of *R*-ratio on fatigue crack growth rates for Westerly granite, tested in the form of three-point bend specimens. (From [Kim 81]; copyright © ASTM; reprinted with permission.)

Comparing this with Eq. 11.10, we see that m is not expected to be affected by R, but C becomes a function of R.

$$C = \frac{C_0}{(1-R)^{m(1-\gamma)}} \tag{11.20}$$

A useful interpretation arising from Eq. 11.18 is that $\overline{\Delta K}$, the equivalent zero-to-tension ($R = 0$) stress intensity, can be plotted versus da/dN, and a single straight line should result. The data of Fig. 11.4 are plotted in this manner in Fig. 11.12, with $\gamma = 0.42$. Since all of the data lie quite close to the single line, the equation is reasonably successful. However, it was necessary to handle loadings involving compression, $R < 0$, by assuming that the compressive portion of the

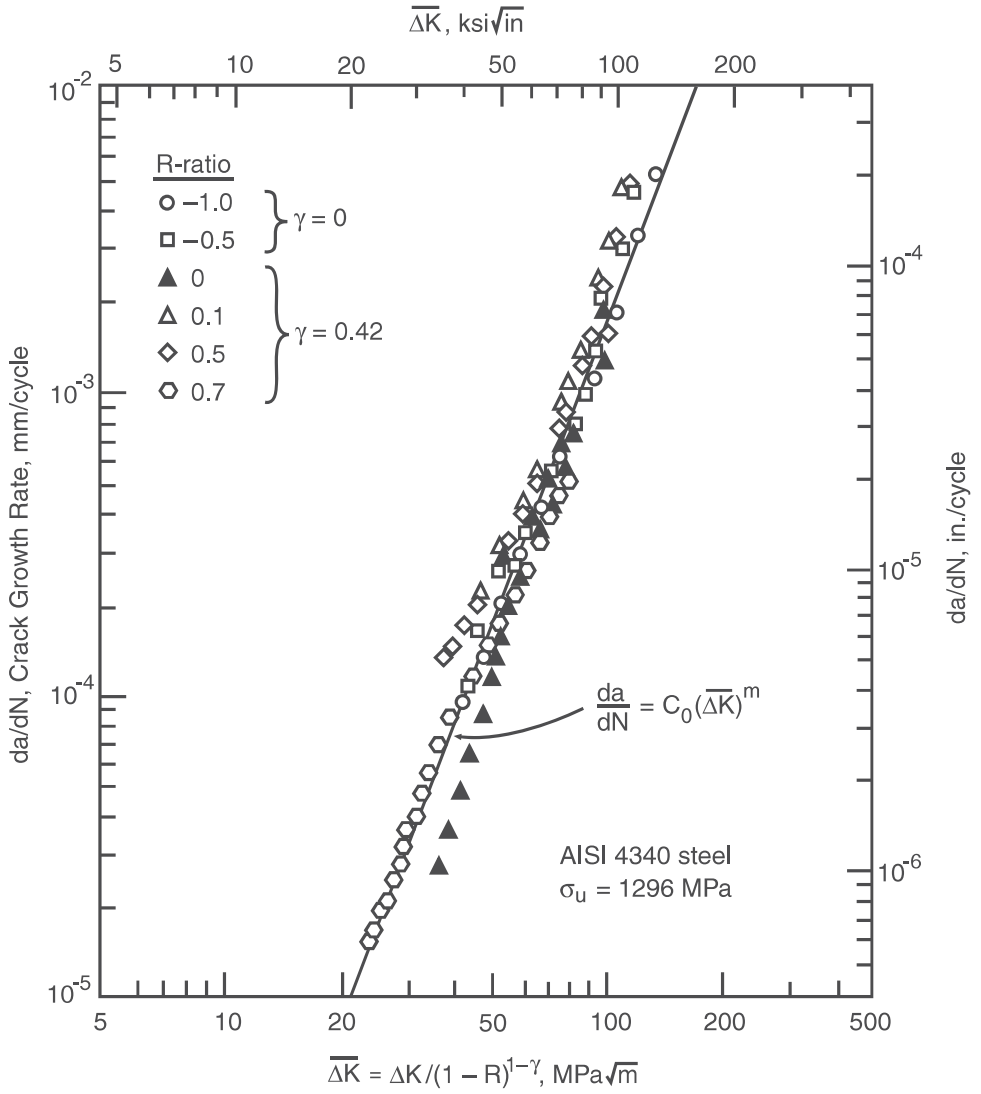

Figure 11.12 Representation of the data of Fig. 11.4 by a single relationship based on the Walker equation. (Data from [Dennis 86].)

cycle had no effect, which is accomplished by using $\gamma = 0$ where $R < 0$, so that $\overline{\Delta K} = K_{max}$. This is reasonable on the basis of the logic that the crack closes at zero load and no longer acts as a crack below this. In more ductile metals, the compressive portion of the loading may contribute to the growth, so this approach is not universally applicable.

Values of the constant γ for various metals are typically around 0.5, but vary from around 0.3 to nearly 1.0. A value of $\gamma = 1$ gives simply $\overline{\Delta K} = \Delta K$, corresponding to no effect of R. Decreasing values of γ imply a stronger effect of R. Constants for the Walker equation are given for several metals in Table 11.2, including the AISI 4340 steel of Fig. 11.12. Where data are available for $R < 0$, note that $\gamma = 0$ applies in three cases, but not for the very ductile Man-Ten steel, for which compressive loading does contribute to crack growth according to $\gamma = 0.22$.

Table 11.2 Constants for the Walker Equation for Several Metals

Material	Yield σ_o	Toughness K_{Ic}	Walker Equation C_0	C_0	m	γ	γ
	MPa (ksi)	MPa $\sqrt{\text{m}}$ (ksi$\sqrt{\text{in}}$)	$\frac{\text{mm/cycle}}{(\text{MPa}\sqrt{\text{m}})^m}$	$\frac{\text{in/cycle}}{(\text{ksi}\sqrt{\text{in}})^m}$		$(R \geq 0)$	$(R < 0)$
Man-Ten steel	363 (52.6)	200[1] (182)	3.28×10^{-9}	1.74×10^{-10}	3.13	0.928	0.220
RQC-100 steel	778 (113)	150[1] (136)	8.01×10^{-11}	4.71×10^{-12}	4.24	0.719	0
AISI 4340 steel ($\sigma_u = 1296$ MPa)	1255 (182)	130 (118)	5.11×10^{-10}	2.73×10^{-11}	3.24	0.420	0
17-4 PH steel (H1050, vac. melt)	1059 (154)	120[1] (109)	3.29×10^{-8}	1.63×10^{-9}	2.44	0.790	—
2024-T3 Al[2]	353 (51.2)	34 (31)	1.42×10^{-8}	7.85×10^{-10}	3.59	0.680	—
7075-T6 Al[2]	523 (75.9)	29 (26)	2.71×10^{-8}	1.51×10^{-9}	3.70	0.641	0

Notes: [1]Data not available; values given are estimates. [2]Values for C_0 include a modification for use in [Hudson 69] of k, where $K = k\sqrt{\pi}$.
Sources: Original data or fitted constants in [Crooker 75], [Dennis 86], [Dowling 79c], [Hudson 69], and [MILHDBK 94] pp. 3–10 and 3–11.

A value of γ can be obtained from data at various R values, the desired γ being the one that best consolidates the data along a single straight line or other curve on a plot of da/dN versus $\overline{\Delta K}$. Where a straight line on a log–log plot is expected, a good initial estimate of γ can be obtained by using the data for two different and contrasting R values, as illustrated in Example 11.3, presented next. However, a more rigorous procedure is to perform a multiple linear regression, starting by taking the logarithm of both sides of Eq. 11.19:

$$\log(da/dN) = m \log(\Delta K) - m(1-\gamma) \log(1-R) + \log C_0 \tag{11.21}$$

The dependent variable is $y = \log(da/dN)$, and the independent ones are $x_1 = \log(\Delta K)$ and $x_2 = \log(1-R)$. See Ex. 10.4 for a similar analysis.

The Walker $\overline{\Delta K}$ in the form of Eq. 11.15 or 11.16 can be used with any mathematical form for the da/dN versus ΔK equation. However, it is primarily employed for intermediate growth rates where Eq. 11.10 does apply.

Example 11.3

Obtain approximate values for the Walker equation constants for the AISI 4340 steel of Fig. 11.4.

Solution Note that the Walker equation assumes that the same exponent m applies for all R-ratios, so that a family of parallel straight lines is formed on a log–log plot. Two such parallel lines for contrasting values of R are sufficient for obtaining approximate values of C_0, m, and γ. The line for $R = 0.1$ already determined in Ex. 11.1 can be used for one of these:

$$\frac{da}{dN} = 2.70 \times 10^{-10}(\Delta K)^{3.46} \qquad (R = 0.1)$$

In this equation and in what follows, units of MPa$\sqrt{\text{m}}$ and mm/cycle are employed. A second line parallel to this one and passing through the $R = 0.7$ data goes approximately through the point

$$\left(\Delta K, \frac{da}{dN}\right) = (11, 10^{-5})$$

The $R = 0.7$ data are roughly parallel to the $R = 0.1$ data, so it is reasonable to proceed with a common $m = 3.46$. The constant C for this second line may be obtained by substituting this m and the preceding point into Eq. 11.10:

$$10^{-5} = C(11)^{3.46}, \qquad C = 2.49 \times 10^{-9}$$

Hence, the equation of the line is

$$\frac{da}{dN} = 2.49 \times 10^{-9}(\Delta K)^{3.46} \qquad (R = 0.7)$$

We now have two values of C, both of which must obey Eq. 11.20.

$$C_{0.1} = \frac{C_0}{(1-R)^{m(1-\gamma)}}, \qquad C_{0.7} = \frac{C_0}{(1-R)^{m(1-\gamma)}}$$

Substituting the respective C and R values, along with the known m, gives two equations with unknowns C_0 and γ:

$$2.70 \times 10^{-10} = \frac{C_0}{(1-0.1)^{3.46(1-\gamma)}}, \qquad 2.49 \times 10^{-9} = \frac{C_0}{(1-0.7)^{3.46(1-\gamma)}}$$

Dividing the second equation into the first eliminates C_0:

$$\frac{2.70 \times 10^{-10}}{2.49 \times 10^{-9}} = \left(\frac{0.3}{0.9}\right)^{3.46(1-\gamma)}$$

Taking logarithms of both sides and solving for γ yields

$$\log \frac{2.70 \times 10^{-10}}{2.49 \times 10^{-9}} = 3.46\,(1-\gamma)\ \log \frac{0.3}{0.9}, \qquad \gamma = 0.415 \qquad \textbf{Ans.}$$

Substituting this γ back into either equation involving C_0 allows that constant to be determined:

$$C_0 = 2.70 \times 10^{-10}(0.9)^{3.46(1-0.415)} = 2.18 \times 10^{-10} \frac{\text{mm/cycle}}{(\text{MPa}\sqrt{\text{m}})^m} \qquad \textbf{Ans.}$$

The final constant is the m value used throughout, $m = 3.46$ (**Ans.**).

Comment These approximate values of the constants agree only roughly with the ones in Table 11.2 for this material, as the latter were fitted by using the full set of data at several R values.

11.4.2 The Forman Equation

Another proposed generalization to include R effects is that of Forman:

$$\frac{da}{dN} = \frac{C_2\,(\Delta K)^{m_2}}{(1-R)\,K_c - \Delta K} = \frac{C_2\,(\Delta K)^{m_2}}{(1-R)\,(K_c - K_{\max})} \tag{11.22}$$

Here, K_c is the fracture toughness for the material and thickness of interest. The second form arises from the first simply by applying Eq. 9.4(a) to ΔK in the denominator. As $K_{\max}$ approaches K_c, the denominator approaches zero, and da/dN becomes large. In particular, there is an asymptote at $\Delta K/(1-R) = K_{\max} = K_c$. The equation thus has the attractive feature of predicting accelerated growth near the final toughness failure, while approaching Eq. 11.10 at low ΔK. Hence, it can be used to fit data that cover both the intermediate and high growth rate regions.

Assuming that crack growth data are available for various R values, we can fit these to Eq. 11.22 by computing the following quantity for each data point:

$$Q = \frac{da}{dN}\,[(1-R)K_c - \Delta K] \tag{11.23}$$

If these Q values are plotted versus the corresponding ΔK values on a log–log plot, a straight line is expected. This is illustrated for 7075-T6 aluminum in Fig. 11.13. The slope of the Q versus ΔK line on the log–log plot is given by m_2, and C_2 is the value of Q at $\Delta K = 1$.

For a given material, the success of the Forman equation can be judged by the extent to which data for various ΔK, R combinations all fall together on a straight line on a log–log plot of Q versus ΔK. For the data of Fig. 11.13(a), the consolidation onto a straight line in (b) is reasonably successful. Constants for the Forman equation corresponding to these data are given in Table 11.3, as are constants for three additional metals.

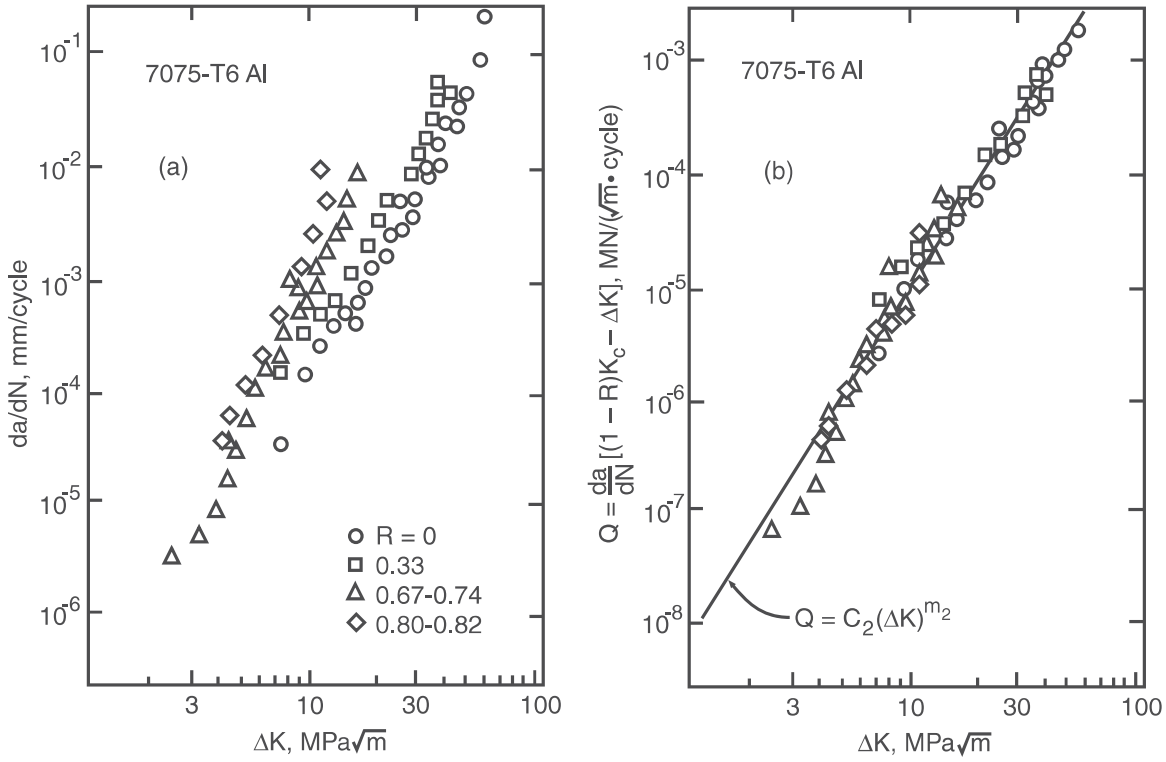

Figure 11.13 Effect of *R*-ratio on growth rates in 7075-T6 aluminum (a), and correlation of these data (b) on the basis of the Forman equation, with constants as listed in Table 11.3. (Data from [Hudson 69].)

11.4.3 Effects on ΔK_{th}

The *R*-ratio generally has a strong effect on the behavior at low growth rates, hence also on the threshold value ΔK_{th}. This occurs even for low-strength metals where there is little effect at intermediate growth rates. Some values of ΔK_{th} for various steels over a range of *R*-ratios are shown in Fig. 11.14. The lower limit of the scatter shown corresponds to ΔK_{th} as follows:

$$\begin{aligned} \Delta K_{th} &= 7.0(1 - 0.85R)\ \text{MPa}\sqrt{\text{m}} \\ &\qquad (R \geq 0.1) \\ \Delta K_{th} &= 6.4(1 - 0.85R)\ \text{ksi}\sqrt{\text{in}} \end{aligned} \tag{11.24}$$

On the basis of the discussion in Barsom (1999), these equations appear to represent a reasonable worst-case estimate for a wide range of steels. However, lower values of ΔK_{th} may apply for highly strengthened steels, which will be illustrated later. Similar trends occur for other classes of metals.

The Walker equation in the form of Eq. 11.15 is sometimes employed to represent the effect of *R*-ratio on ΔK_{th} for a given material:

$$\Delta K_{th} = \overline{\Delta K}_{th}(1 - R)^{1-\gamma_{th}} \tag{11.25}$$

Table 11.3 Constants for the Forman Equation for Several Metals

Material	Yield σ_o	Toughness K_{Ic}	Forman Equation C_2	C_2	m_2	K_c
	MPa (ksi)	$\text{MPa}\sqrt{\text{m}}$ ($\text{ksi}\sqrt{\text{in}}$)	$\frac{\text{mm/cycle}}{(\text{MPa}\sqrt{\text{m}})^{m_2-1}}$	$\frac{\text{in/cycle}}{(\text{ksi}\sqrt{\text{in}})^{m_2-1}}$		$\text{MPa}\sqrt{\text{m}}$ ($\text{ksi}\sqrt{\text{in}}$)
17-4 PH steel (H1025)	1145 (166)	—	1.40×10^{-6}	6.45×10^{-8}	2.65	132 (120)
Inconel 718 (Fe-Ni-base, aged)	1172 (170)	132 (120)	4.29×10^{-6}	2.00×10^{-7}	2.79	132 (120)
2024-T3 Al[1]	353 (51.2)	34 (31)	2.31×10^{-6}	1.14×10^{-7}	3.38	110 (100)
7075-T6 Al[1]	523 (75.9)	29 (26)	5.29×10^{-6}	2.56×10^{-7}	3.21	78.7 (71.6)

Notes: [1]Values for C_2 and K_c include a modification for use in [Hudson 69] of k, where $K = k\sqrt{\pi}$. The K_c values are for 2.3 mm thick sheet material; replace with K_{Ic} for thick material.
Sources: Values in [Hudson 69], [MILHDBK 94] pp. 2–198 and 6–59, and [Smith 82].

Here, $\overline{\Delta K}_{th}$ and γ_{th} are empirical constants fitted to test data of ΔK_{th} values for various R. Note that $\overline{\Delta K}_{th}$ corresponds to ΔK_{th} at $R = 0$. Values of γ_{th} will not generally agree with γ fitted to the Walker equation in the intermediate growth rate region. In particular, there is usually an increased sensitivity to R-ratio in the low growth rate and threshold region.

11.4.4 Discussion

A variety of other mathematical expressions, some of them quite complex, have been used to represent da/dN versus ΔK curves. Some of these are not merely empirical, but are based on attempts to include modeling of the closing of the crack and other physical phenomena that affect crack growth. Many give a curve shape similar to Fig. 11.3, where the curve steepens at both low and high growth rates. If R-ratio effects are included and the da/dN versus ΔK behavior ranges over the regions of low, intermediate, and high growth rates, as many as 10 empirical constants may be required to accurately represent the behavior of a given material.

An alternative to curve fitting with empirical constants is to use a *table lookup procedure*. In this case, numerical data of da/dN versus ΔK for various R-ratios are maintained in tabular form in a digital computer, and interpolation is employed to determine da/dN for a desired combination of ΔK and R. For additional detail on representing da/dN versus ΔK behavior, see Forman (2005), Grandt (2004), and Henkener (1993).

A simple, but approximate, approach to representing da/dN versus ΔK behavior is illustrated in Fig. 11.15. In the intermediate region, use the Walker relationship, Eq. 11.19, with appropriately fitted materials constants C_0, m, and γ. Then in the threshold region, assume that there is an abrupt

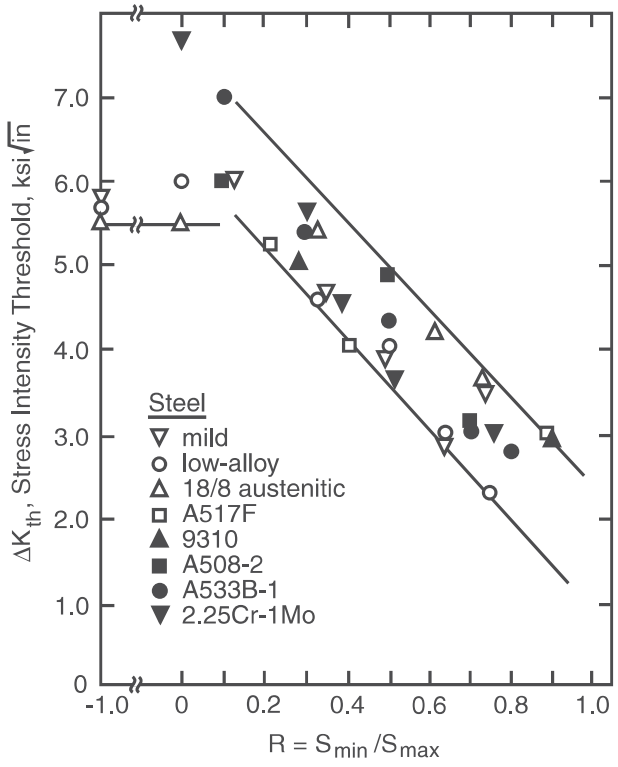

Figure 11.14 Effect of *R*-ratio on the threshold ΔK_{th} for various steels. For $R = -1$, the compressive portion of the loading cycle is here excluded from calculations of ΔK_{th}. (Adapted from [Barsom 87] p. 285; © 1987 by Prentice Hall, Upper Saddle River, NJ; reprinted with permission.)

transition to a vertical limit, ΔK_{th}, as given by Eq. 11.25 or other analogous relationship. Additional materials constants, such as $\overline{\Delta K_{th}}$ and γ_{th}, are then needed. However, it is conservative to simply ignore the threshold, as shown by the dashed line. Finally, represent the unstable rapid-growth-rate region as another vertical limit. This limit occurs upon reaching either the fracture toughness or the fully plastic limit load, the latter occurring due to the decreasing cross-sectional area of the cracked member. Either of these may occur first.

A situation often encountered is that data for a material of interest are available only for zero-to-tension or similar loading—that is, for R in the range 0 to 0.2. For engineering metals in the intermediate growth rate region, it is reasonable to employ such data with the Walker equation by assuming a value of $\gamma = 0.5$. This will generally provide a conservative estimate of the behavior at other positive R-ratios.

The use of a fracture toughness constant K_c in the Forman and other crack growth equations is necessary for accurate representation of behavior at high growth rates. However, some care is needed. First, K_c varies with thickness unless the behavior is plane strain, where K_{Ic} applies. In addition, the severe cyclic loading that occurs just prior to brittle fracture at the end of a crack growth test may alter K_c, increasing it for certain materials and decreasing it for others. Further, for ductile, high-toughness materials such as mild steel, fatigue crack growth tests may terminate due to gross yielding instead of brittle fracture. It is then not appropriate to obtain a K_c value from such data.

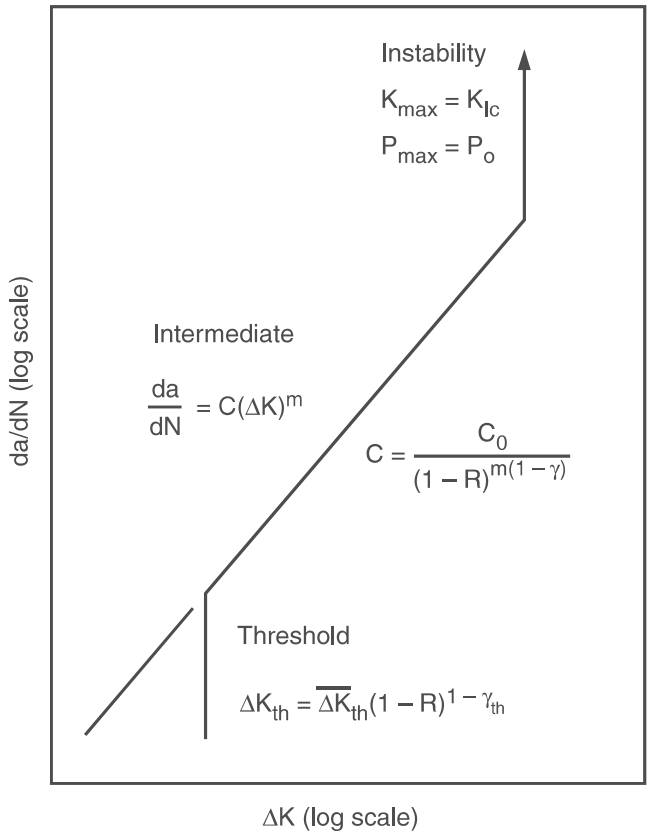

Figure 11.15 Approximate representation of da/dN versus ΔK behavior with R-ratio effects included. The Walker equation is used for the intermediate region, along with a possible threshold limit at low growth rates. There is also an instability limit at high growth rates, due to either brittle fracture or fully plastic yielding.

11.5 TRENDS IN FATIGUE CRACK GROWTH BEHAVIOR

Fatigue crack growth behavior differs considerably for different classes of material. It is also affected, sometimes to a large extent, by changes in the environment, such as temperature or hostile chemicals.

11.5.1 Trends with Material

The crack growth behavior in air at room temperature may vary only modestly within a narrowly defined class of materials. For example, data for $R \approx 0$ for several ferritic-pearlitic steels are shown in Fig. 11.16. An equation of the form of Eq. 11.10 is shown that represents the worst case for the several steels tested, with this equation corresponding to the constants given in Table 11.1. Recall from Chapter 3 that ferritic-pearlitic steels have low carbon contents and are relatively low-strength steels used for structural members, pressure vessels, and similar applications.

Worst-case da/dN versus ΔK equations are given in Barsom (1999) for two additional classes of steel, namely, martensitic steels and austenitic stainless steels. The constants have already been presented in Table 11.1. Martensitic steels are distinguished as being steels that are heat treated by

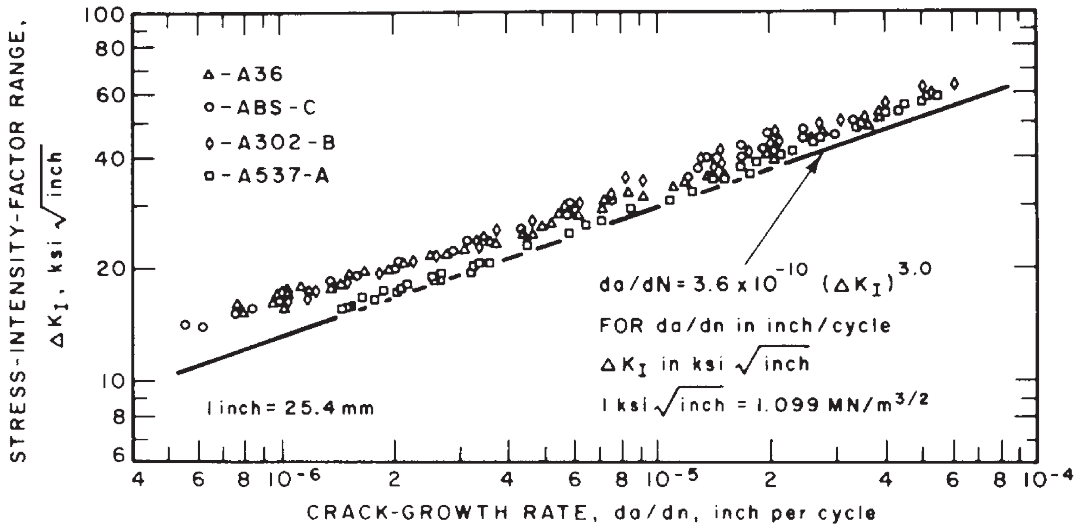

Figure 11.16 Fatigue crack growth rate data at $R \approx 0$ for four ferritic-pearlitic steels, and a line giving worst-case growth rates. Note that the axes are reversed, compared with the other da/dN versus ΔK plots given. (From [Barsom 71]; used with permission of ASME.)

quenching and tempering, so this group includes many low-alloy steels, and also those 400-series stainless steels with less than 15% Cr. Austenitic steels are primarily the 300-series stainless steels, which are used where corrosion resistance is critical. These equations apply for R values near zero, say, up to $R = 0.2$. For higher R-ratios, it is suggested that these constants be employed as C_0 and m in the Walker equation, along with an assumed value of $\gamma = 0.5$.

These general-purpose equations need to be used with some care, as exceptions do exist where they are not very accurate. For example, if the widely used martensitic steel AISI 4340 is heat treated to various strength levels, including very high strength levels, the crack growth rates may exceed the suggested worst-case trend. In addition, the ΔK_{th} values for high-strength steels may be considerably below the typical behavior of Fig. 11.14. Test data showing the trend of ΔK_{th} with strength level in AISI 4340 steel are given in Fig. 11.17. The decrease in ΔK_{th} with strength parallels the similar trend in fracture toughness for this material. (See Fig. 8.32.)

If various major classes of metals are considered, such as steels, aluminum alloys, and titanium alloys, crack growth rates differ considerably when compared on a da/dN versus ΔK plot. However, the ΔK values corresponding to a given growth rate scale roughly with the elastic modulus E. Hence, a plot of da/dN versus $\Delta K/E$ removes much of the difference among various metals, as shown in Fig. 11.18. Polymers exhibit a wide range of growth rates when compared on the basis of ΔK, as shown in Fig. 11.19. For any given ΔK level, the growth rates are considerably higher than for most metals.

One generalization that may be made is that the crack growth rate exponent m is higher for lower ductility (more brittle) materials. For ductile metals, m is typically in the range 2 to 4 and is often around 3. Higher exponents occur for more brittle cast metals, for short-fiber reinforced composites, and for ceramics, including concrete. For example, m is near 12 for the granite rock of Fig. 11.11.

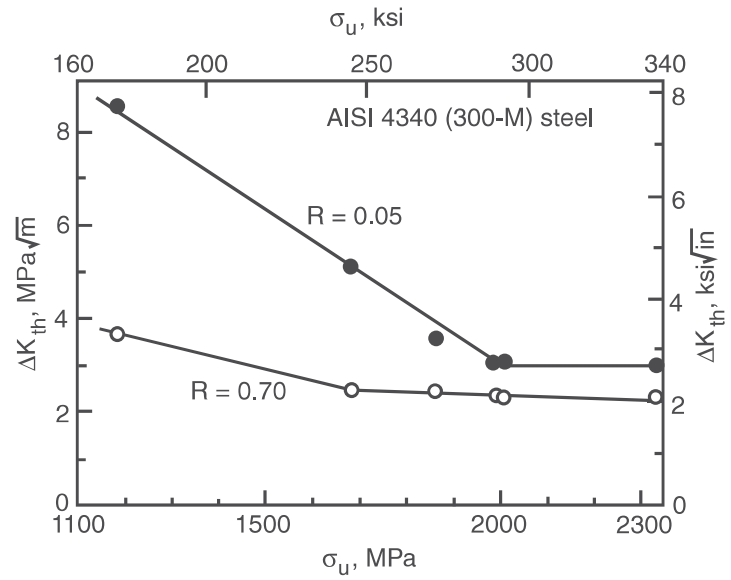

Figure 11.17 Effect of strength level of an alloy steel on ΔK_{th} at two R-ratios. (Adapted from [Ritchie 77]; used with permission of ASME.)

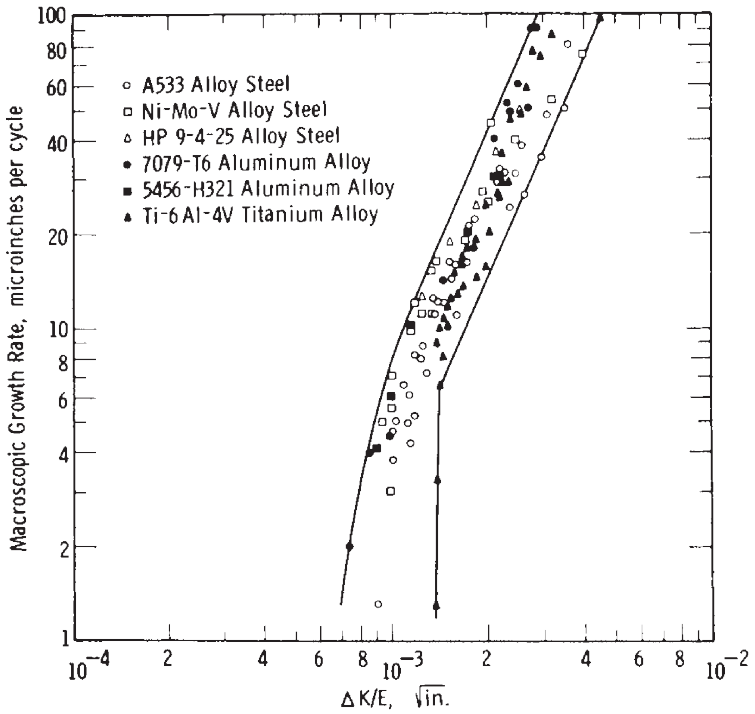

Figure 11.18 Fatigue crack growth trends for various metals correlated by plotting $\Delta K/E$. (From [Bates 69]; used with permission.)

Despite the generalizations that may be made as to similar behavior within classes of materials, surprisingly small differences can sometimes have a significant effect. For example, decreasing the grain size in steels has the detrimental effect of lowering ΔK_{th}, while the behavior outside of the low

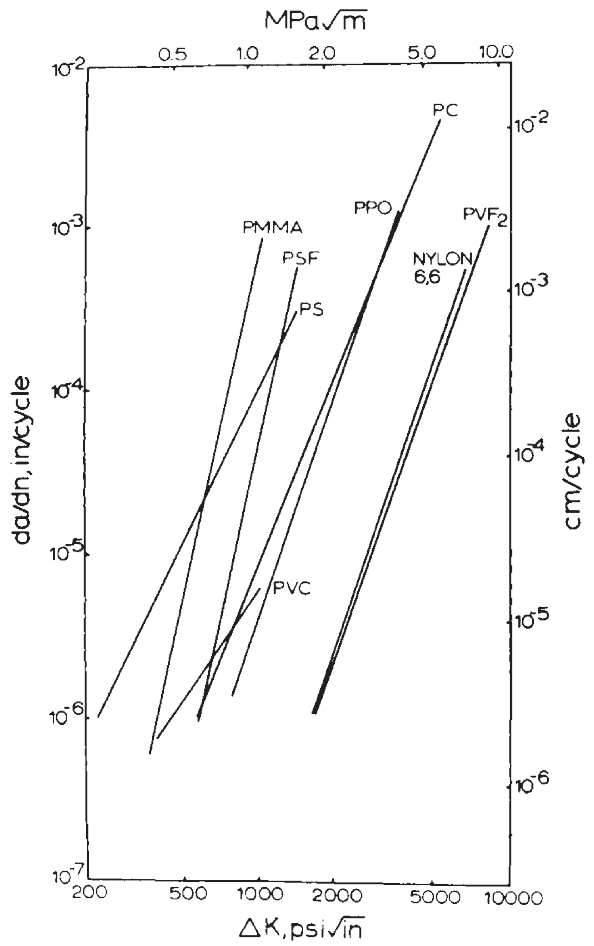

Figure 11.19 Fatigue crack growth trends for various crystalline and amorphous polymers. (From [Hertzberg 75]; used with permission.)

growth rate region is relatively unaffected. Also, as might be expected, variations in reinforcement often have a significant effect on crack growth in composites materials, an example of which is given in Fig. 11.20.

11.5.2 Trends with Temperature and Environment

Changing the temperature usually affects the fatigue crack growth rate, with higher temperature often causing faster growth. Data illustrating such behavior for the austenitic (FCC) stainless steel AISI 304 are shown in Fig. 11.21 (left). However, an opposite trend can occur in BCC metals due to the cleavage mechanism contributing to fatigue crack growth at low temperature. (See Section 8.6.) Such a trend for an Fe-21Cr-6Ni-9Mn alloy is illustrated in Fig. 11.21 (right). This alloy is austenitic at room temperature, but at low temperatures it is martensitic (BCC), and hence subject to cleavage, so that the more usual temperature effect is reversed. The effect of this cleavage contribution in BCC irons and steels can have a large effect on the fatigue crack growth exponent m, as shown in Fig. 11.22. Suppressing this effect by adding sufficient nickel avoids high growth rates at low temperature.

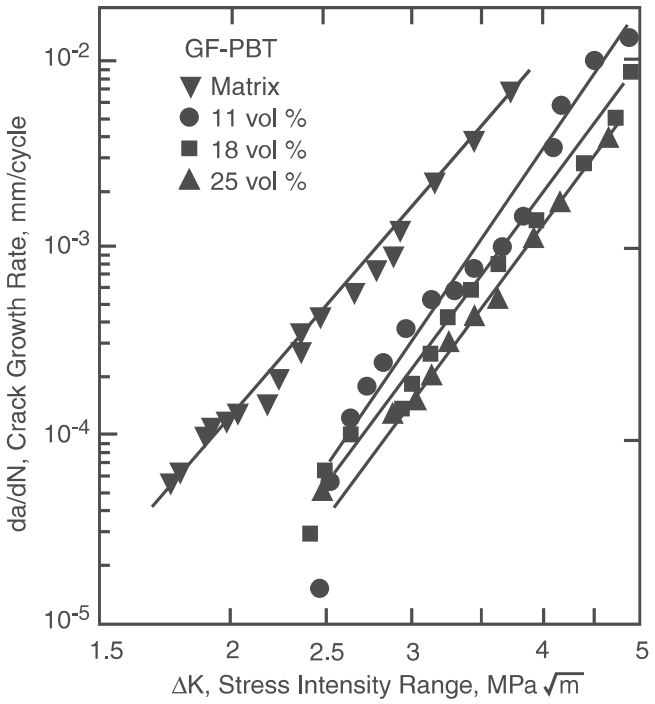

Figure 11.20 Effect on crack growth rates at $R = 0.2$ of various amounts of short glass fibers, in a matrix of the thermoplastic polymer PBT, with crack propagation perpendicular to the mold-fill direction. (Adapted from [Voss 88]; used with permission.)

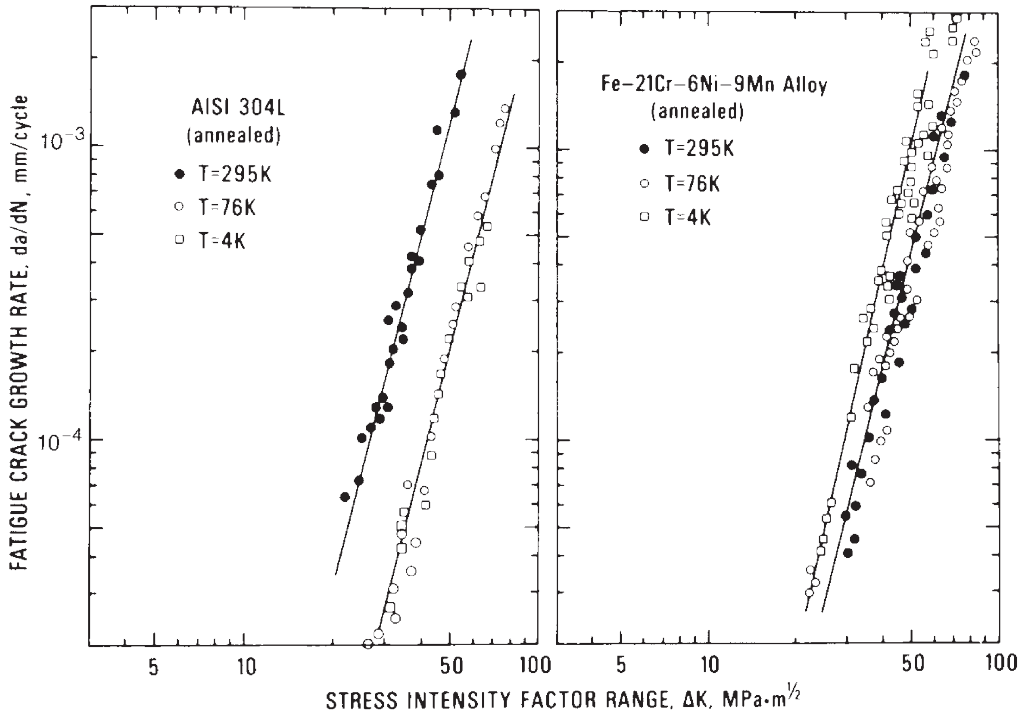

Figure 11.21 Effect of temperature on fatigue crack growth rates in two metals. (From [Tobler 78]; used with permission.)

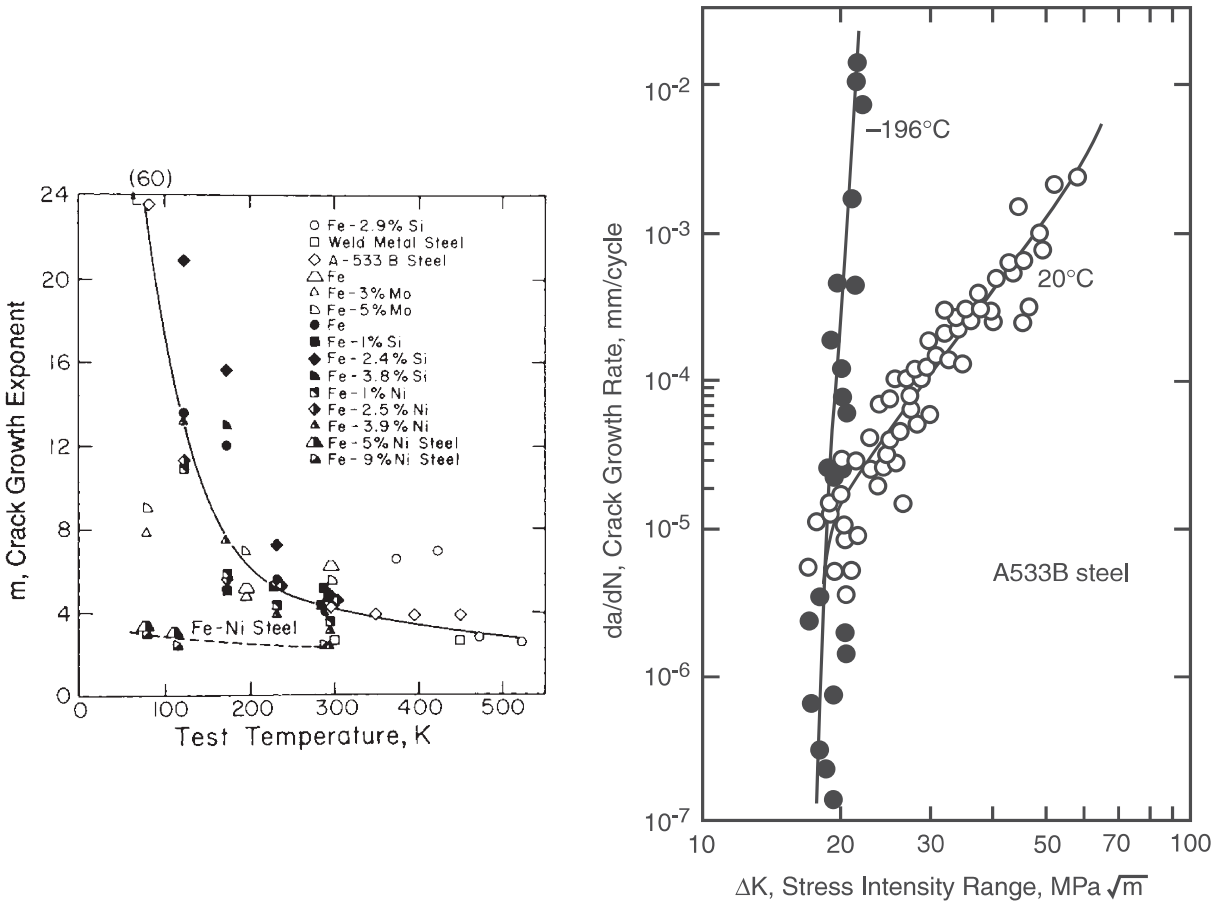

Figure 11.22 Variation (left) of the exponent m for the Paris equation with test temperature for iron and various steels at R-ratios near zero. Shown on the right is the associated drastic increase in growth rates at low temperature for A533B steel tested at $R = 0.1$. (Left from [Gerberich 79]; copyright © ASTM; reprinted with permission. Right adapted from [Campbell 82] p. 83, as based on data from [Stonesifer 76]; used with permission.)

Hostile chemical environments often increase fatigue crack growth rates, with certain combinations of material and environment causing especially large effects. The term *corrosion fatigue* is often used when the environment involved is a corrosive medium, such as seawater. Such behavior is illustrated in Fig. 11.23, which shows the effect of a saltwater solution similar to seawater on two strength levels of AISI 4340 steel. The effect is considerably greater for the higher strength level of this steel. The effect on growth rate per cycle, da/dN, of a given hostile environment is usually greater at slower frequencies of cycling, where the environment has more time to act. This trend is apparent in the data of Fig. 11.24.

Even the gases and moisture in air can act as a hostile environment, which can be demonstrated by comparing test data in vacuum or an inert gas with data in air. Such comparisons for a metal and a ceramic are shown in Fig. 11.25. This circumstance results in frequency effects occurring in ambient air for some materials. Since chemical activity increases with temperature, the general trend of increasing growth rate with temperature is explained, at least in part, by the ambient air having a hostile effect.

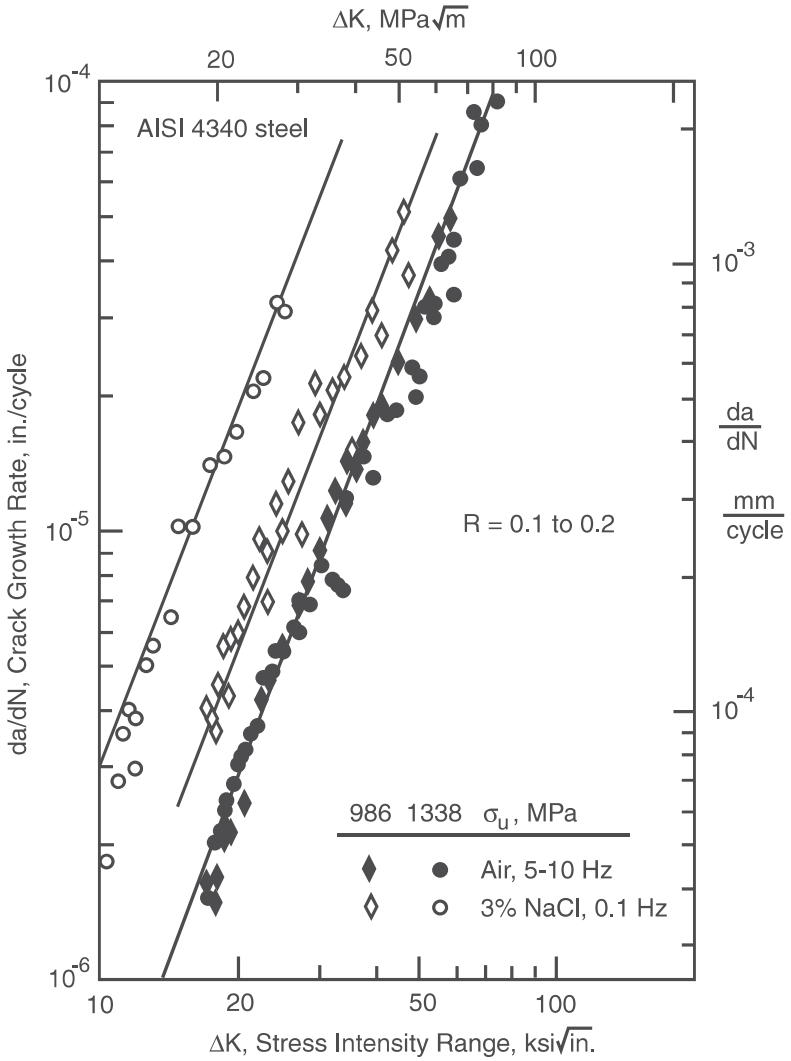

Figure 11.23 Contrasting sensitivity to corrosion fatigue crack growth of two strength levels of an alloy steel. (Adapted from [Imhof 73]; copyright © ASTM; reprinted with permission.)

11.6 LIFE ESTIMATES FOR CONSTANT AMPLITUDE LOADING

Since ΔK increases with crack length during constant amplitude stressing ΔS, and since the crack growth rate da/dN depends on ΔK, the growth rate is not constant, but increases with crack length. In other words, the crack accelerates as it grows, as for the data of Fig. 11.8. This situation of changing da/dN necessitates the use of an integration procedure to obtain the life required for crack growth.

Crack growth rates da/dN for a given combination of material and R-ratio are given as a function of ΔK by Eqs. 11.10, 11.18, and 11.22, and by other similar equations, which may be represented in general by

$$\frac{da}{dN} = f\,(\Delta K, R) \tag{11.26}$$

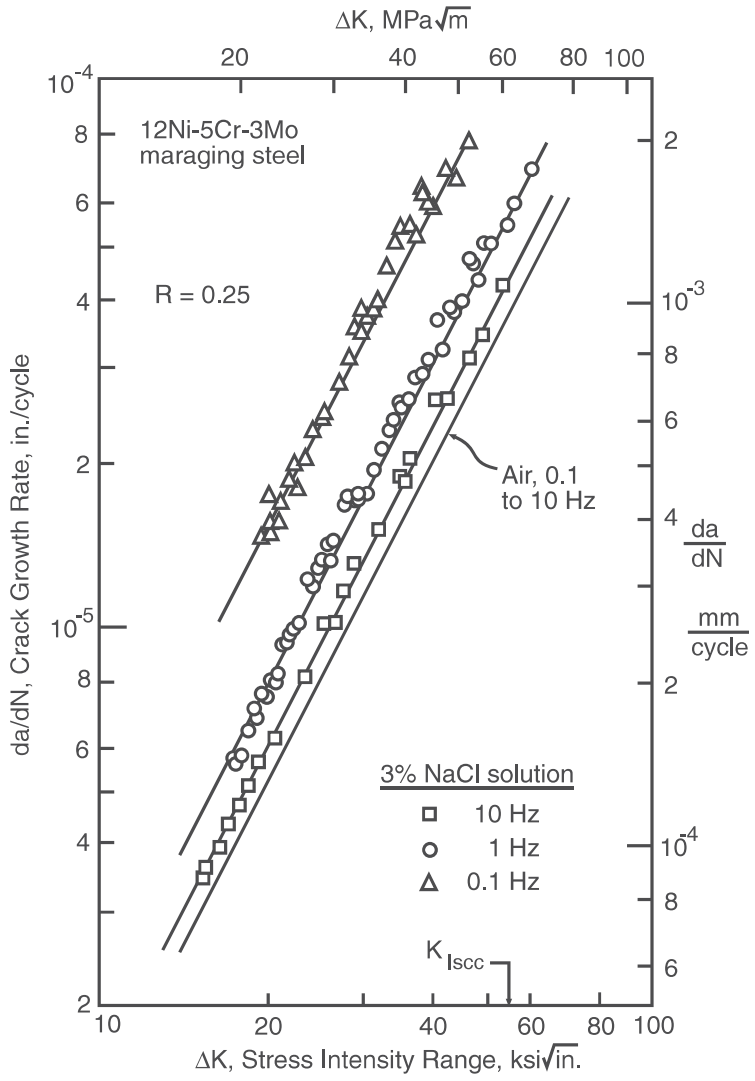

Figure 11.24 Frequency effects on corrosion fatigue crack growth rates in a maraging steel. (Adapted from [Imhof 73]; copyright © ASTM; reprinted with permission.)

where any effects of environment, frequency, etc., are assumed to be included in the material constants involved. The life in cycles required for crack growth may be calculated by solving this equation for dN and integrating both sides:

$$\int_{N_i}^{N_f} dN = N_f - N_i = N_{if} = \int_{a_i}^{a_f} \frac{da}{f\,(\Delta K, R)} \tag{11.27}$$

This integral gives the number of cycles required for the crack to grow from an initial size a_i at cycle number N_i to a final size a_f at cycle number N_f. It is convenient to use the symbol N_{if} to represent the number of elapsed cycles, $N_f - N_i$.

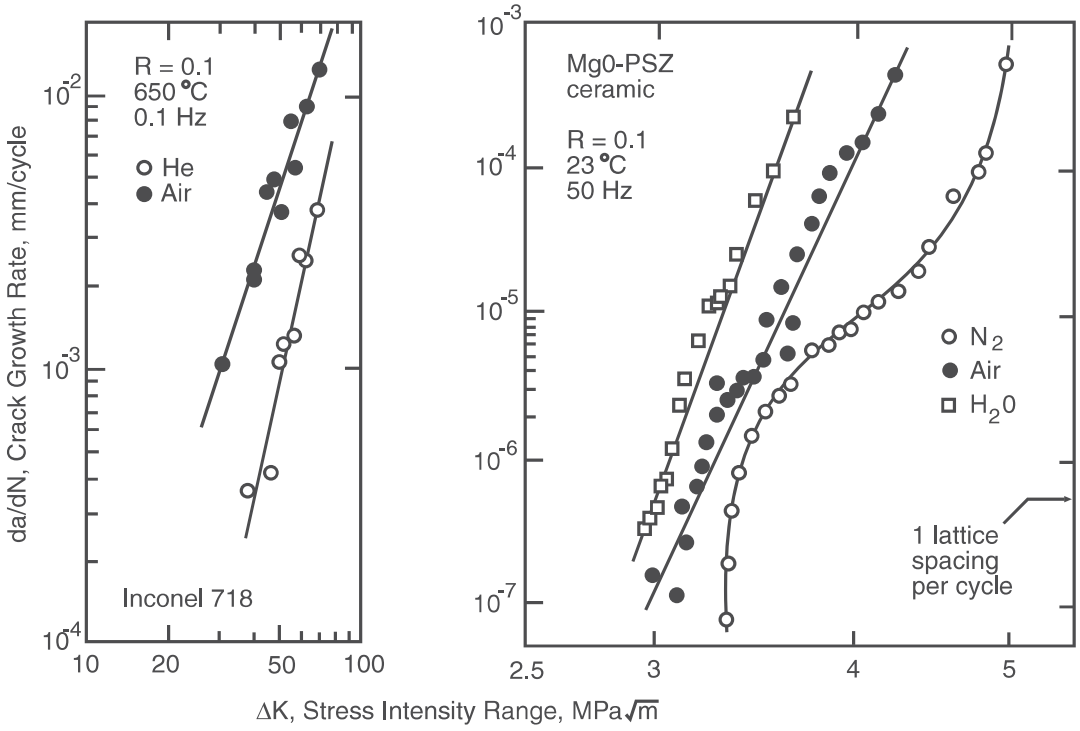

Figure 11.25 Faster fatigue crack growth in air than in inert gas (left) for the Ni-base alloy Inconel 718 at elevated temperature, and (right) for a magnesia, partially stabilized zirconia ceramic. (Left adapted from [Floreen 79]; used with permission. Right adapted from [Dauskardt 90]; reprinted by permission of the American Ceramic Society.)

The inverse of the growth rate, dN/da, is the rate of accumulation of cycles, N, per unit increase in crack length a. From Eq. 11.26, this is given by

$$\frac{dN}{da} = \frac{1}{da/dN} = \frac{1}{f(\Delta K, R)} \tag{11.28}$$

Note that Eq. 11.27 can also be written

$$N_{if} = \int_{a_i}^{a_f} \left(\frac{dN}{da}\right) da \tag{11.29}$$

Hence, if dN/da from Eq. 11.28 is plotted as a function of a, the life N_{if} is given by the area under this curve between a_i and a_f. This is illustrated in Fig. 11.26.

To perform the integration for a particular case, it is necessary to substitute the specific da/dN equation for the material and R of interest, and also the specific equation for ΔK for the geometry of interest. Some useful closed-form solutions exist, but numerical integration is necessary in many cases.

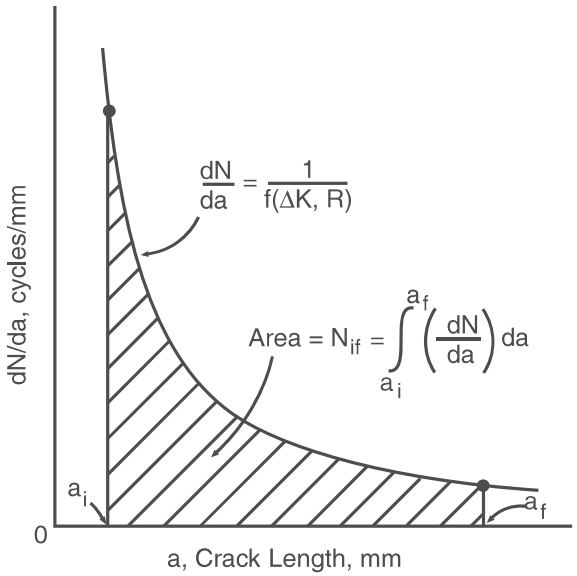

Figure 11.26 Area under the dN/da versus a curve used to estimate the number of cycles to grow a crack from initial size a_i to final size a_f.

11.6.1 Closed-Form Solutions

Consider a situation where growth rates are given by Eq. 11.10 and where $F = F(a/b)$ in Eq. 11.7 can be approximated as constant over the range of crack lengths a_i to a_f:

$$\frac{da}{dN} = f\,(\Delta K, R) = C\,(\Delta K)^m, \qquad \Delta K = F\,\Delta S\sqrt{\pi a} \tag{11.30}$$

The value of C used can include the effect of the ratio $R = S_{\min}/S_{\max}$, as from the Walker approach using Eq. 11.20. Assume that $S_{\max}$ and $S_{\min}$ are constant, so that ΔS and R are also both constant. Substituting this particular $f(\Delta K, R)$ into Eq. 11.27 and then substituting for ΔK gives

$$N_{if} = \int_{a_i}^{a_f} \frac{da}{C\,(\Delta K)^m} = \int_{a_i}^{a_f} \frac{da}{C\left(F\,\Delta S\sqrt{\pi a}\right)^m} = \int_{a_i}^{a_f} \frac{1}{C\left(F\,\Delta S\sqrt{\pi}\right)^m} \frac{da}{a^{m/2}} \tag{11.31}$$

Since C, F, ΔS, and m are all constant, the only variable is a, and integration is straightforward, giving

$$N_{if} = \frac{a_f^{1-m/2} - a_i^{1-m/2}}{C\left(F\,\Delta S\sqrt{\pi}\right)^m (1 - m/2)} \qquad (m \neq 2) \tag{11.32}$$

If $m = 2$, this equation is mathematically indeterminate.

Where a_f is substantially larger than a_i and m is around 3 or greater, the a_i term dominates the numerator of Eq. 11.32, and the life is insensitive to the value of a_f. This trend is accentuated for larger values of m. With reference to Fig. 11.26, the area under the curve, N_{if}, is affected only a small amount by the exact choice of a_f. Also, since most of the area, and thus most of the cycles, are accumulated near a_i, the value of constant F chosen for Eq. 11.32 should be closer to the value

F_i corresponding to a_i than to the value F_f corresponding to a_f. Hence, either use F_i or a slightly higher intermediate value.

Additional closed-form solutions exist that may be useful, such as one for the case of $m = 2$, with derivations of some of these being included as Problems at the end of this chapter. However, where $F = F(a/b)$ must be treated as a variable, the variety of these is severely limited due to the appearance of m as an exponent on F in the denominator of Eq. 11.31.

The preceding equations assume constant amplitude loading, so the gross section nominal stresses $S_{\max}$ and $S_{\min}$ are constant during cycling. If these change, the integral of Eq. 11.27, and any equations obtained from it, can be used in separate calculations for periods of crack growth during which the load levels are constant. The cycle numbers for each of these periods can then be summed to obtain the total life. However, see the additional discussion of variable amplitude loading given later in Section 11.7.

11.6.2 Crack Length at Failure

In employing Eq. 11.27 to estimate crack growth life, the final crack length a_f is often unknown and must be determined before the equation can be applied. In addition, if F is taken as constant, as in Eq. 11.32, it is also necessary to determine $F_f = F(a_f/b)$, so that it can be confirmed that this value does not differ excessively from $F_i = F(a_i/b)$. If F_f and F_i differ by more than about 15 to 20%, the resulting error in N_{if} due to using a constant value will generally be unacceptably large. Numerical integration, as described in Section 11.6.3, is then usually needed.

Under constant amplitude cyclic loading, the value $K_{\max}$ corresponding to $S_{\max}$ increases as crack growth proceeds. When $K_{\max}$ reaches the fracture toughness K_c for the material and thickness of interest, failure is expected at the length a_c that is critical for brittle fracture:

$$a_c = \frac{1}{\pi}\left(\frac{K_c}{F S_{\max}}\right)^2 \tag{11.33}$$

Since F varies, a graphical or iterative solution as already illustrated by Example 8.1(c) is generally needed to obtain a_c.

In addition, crack growth causes a loss of cross-sectional area, and thus an increase in the stress on the remaining uncracked (net) area. Depending on the material and the member geometry and size, fully plastic yielding may be reached prior to $K_{\max} = K_c$. This is most likely for ductile materials with low strength and high fracture toughness. Hence, a_f is the smaller of two possibilities, a_c and a_o, where the latter is the crack length corresponding to fully plastic yielding. Values of a_o may be estimated on the basis of fully plastic behavior, as discussed in Appendix A, Section A.7.2. For some simple two-dimensional cases, useful equations for a_o obtained in this manner are given in Fig. A.16.

Use of linear-elastic fracture mechanics up to the crack length a_o corresponding to fully plastic yielding violates the plastic zone size limitations of LEFM, as discussed in Chapter 8. The effect of yielding just prior to reaching a_o will be to increase growth rates to higher values than those calculated, giving an actual life that is shorter than calculated. However, recall from Fig. 11.26 that cracks accelerate during their growth, so most cycles are exhausted while the crack is short, and few are spent while the crack is near its final length. The error in life from this source is thus usually

small, so the suggested procedure of choosing the smaller of a_c and a_o is useful and appropriate as an approximation for engineering purposes.

Another source of possible error in life estimates is that the fracture toughness K_c at the end of cyclic loading may differ from standard values obtained in static tests. However, if a_f is significantly larger than a_i, the effect on life of an altered value of K_c may not be large, which also arises from the situation illustrated by Fig. 11.26.

Example 11.4

A center-cracked plate of the AISI 4340 steel ($\sigma_u = 1296\,\text{MPa}$) of Table 11.2 has dimensions, as defined in Fig. 8.12(a), of $b = 38$ and $t = 6\,\text{mm}$, and it contains an initial crack of length $a_i = 1\,\text{mm}$. It is subjected to tension-to-tension cyclic loading between constant values of minimum and maximum force, $P_{\min} = 80$ and $P_{\max} = 240\,\text{kN}$.

(a) At what crack length a_f is failure expected? Is the cause of failure yielding or brittle fracture?
(b) How many cycles can be applied before failure occurs?
(c) Assume that this member is an engineering component that is expected to be subjected to 150,000 cycles in its service life, and further assume that a safety factor of three on life is required. If $a_i = 1\,\text{mm}$ is the minimum detectable crack length a_d for inspection, are periodic inspections required? If so, at what interval?
(d) Consider the possibility of avoiding periodic inspections by improved initial inspection, such that a smaller a_i can be justified. What new $a_i = a_d$ would be required?

Solution **(a)** The crack length at fully plastic yielding can be estimated from Fig. A.16(a):

$$a_o = b\left(1 - \frac{P_{\max}}{2bt\sigma_o}\right) = (38\,\text{mm})\left(1 - \frac{240{,}000\,\text{N}}{2(38\,\text{mm})(6\,\text{mm})(1255\,\text{MPa})}\right) = 22.1\,\text{mm}$$

The yield strength (and also K_{Ic}) is obtained from Table 11.2.

The crack length a_c at brittle fracture is given by Eq. 11.33:

$$a_c = \frac{1}{\pi}\left(\frac{K_{Ic}}{FS_{\max}}\right)^2$$

With reference to Fig. 8.12(a), an initial estimate of a_c may be made by assuming that $a_c/b \leq 0.4$, so that $F \approx 1$. We obtain

$$S_{\max} = \frac{P_{\max}}{2bt} = \frac{240{,}000\,\text{N}}{2(38\,\text{mm})(6\,\text{mm})} = 526\,\text{MPa}$$

$$a_c \approx \frac{1}{\pi}\left(\frac{K_{Ic}}{FS_{\max}}\right)^2 = \frac{1}{\pi}\left(\frac{130\,\text{MPa}\sqrt{\text{m}}}{1(526\,\text{MPa})}\right)^2 = 0.0194\,\text{m} = 19.4\,\text{mm}$$

Table E11.4

Calc. No.	Trial a mm	$\alpha = a/b$	F	$K_{\max} = FS_{\max}\sqrt{\pi a}$ MPa$\sqrt{\text{m}}$
1	15	0.395	1.097	125.3
2	16	0.421	1.114	131.3
3	15.77	0.416	1.110	130.0

This corresponds to $a_c/b = 0.51$, which is beyond the region of 10% accuracy for $F \approx 1$. A trial and error solution, as in Ex. 8.1(c), is thus needed, with F taken from Fig. 8.12(a). This is shown in Table E11.4. The final K value is $K_{Ic} = 130\,\text{MPa}\sqrt{\text{m}}$ so that $a_c = 15.8\,\text{mm}$. Since this is smaller than a_o, brittle fracture determines the controlling value a_f, and

$$a_f = 15.8\,\text{mm} \qquad \textbf{Ans.}$$

(b) If F is approximately constant, Eq. 11.32 can be employed to calculate N_{if} by substituting either the initial F or an intermediate value that is biased toward the initial one:

$$N_{if} = \frac{a_f^{1-m/2} - a_i^{1-m/2}}{C\left(F\,\Delta S\sqrt{\pi}\right)^m (1 - m/2)}$$

In this case, the value increases from $F_i = 1.00$ to $F_f = 1.11$. So the variation is small enough that constant F is a reasonable assumption, and we can use $F = 1.00$ for the N_{if} calculation. If we note that Table 11.2 gives constants for the Walker equation, we see that the nonzero R-ratio for the applied load can be handled by calculating a C value from Eq. 11.20 as follows:

$$R = \frac{S_{\min}}{S_{\max}} = \frac{P_{\min}}{P_{\max}} = \frac{80}{240} = 0.333$$

$$C = \frac{C_0}{(1-R)^{m(1-\gamma)}} = \frac{5.11 \times 10^{-10}}{(1 - 0.333)^{3.24(1-0.42)}} = 1.095 \times 10^{-9}\,\frac{\text{mm/cycle}}{(\text{MPa}\sqrt{\text{m}})^m}$$

However, substitution into the equation for N_{if} is most convenient if all quantities have units consistent with MPa$\sqrt{\text{m}}$ as used for ΔK, requiring a units conversion for C as follows:

$$C = 1.095 \times 10^{-9}\,\frac{\text{mm/cycle}}{(\text{MPa}\sqrt{\text{m}})^m} \times \frac{1\text{ m}}{1000\text{ mm}} = 1.095 \times 10^{-12}\,\frac{\text{m/cycle}}{(\text{MPa}\sqrt{\text{m}})^m}$$

Two additional calculations are useful before computing N_{if}:

$$\Delta S = S_{\max}(1 - R) = 526(0.667) = 351\,\text{MPa}$$

$$\left(1 - \frac{m}{2}\right) = \left(1 - \frac{3.24}{2}\right) = -0.62$$

Substituting the various numerical values finally gives N_{if}:

$$N_{if} = \frac{(0.0158\text{ m})^{-0.62} - (0.001\text{ m})^{-0.62}}{\left(1.095 \times 10^{-12} \dfrac{\text{m/cycle}}{(\text{MPa}\sqrt{\text{m}})^m}\right)(1.00 \times 351\,\text{MPa} \times \sqrt{\pi})^{3.24}(-0.62)}$$

$$N_{if} = 77{,}600 \text{ cycles} \qquad \textbf{Ans.}$$

In the preceding substitutions, note that all units are meters, MPa, or combinations of these. Careful checking indicates that these all cancel, leaving only "cycles."

(c) With no periodic inspections, the safety factor on life from Eq. 11.2 is

$$X_N = \frac{N_{if}}{\hat{N}} = \frac{77{,}600}{150{,}000} = 0.52$$

Hence, failure is expected before the end of the service life, so inspections are clearly needed. For the required $X_N = 3$, the inspection interval can be obtained from Eq. 11.5:

$$N_p = \frac{N_{if}}{X_N} = \frac{77{,}600}{3} = 25{,}900 \text{ cycles} \qquad \textbf{Ans.}$$

(d) To avoid periodic inspections and satisfy $X_N = 3$, we need a new, smaller $a_i = a_d$ such that N_{if} is

$$N_{if} = X_N \hat{N} = 3(150{,}000) = 450{,}000 \text{ cycles}$$

Equation 11.32 is needed again, but now with N_{if} known and a_i unknown. Noting that the same values of a_f, C, m, F, and ΔS apply as in (b), and handling units as before, we have the following substitutions:

$$450{,}000 = \frac{(0.0158)^{-0.62} - a_i^{-0.62}}{(1.095 \times 10^{-12})(1.00 \times 351\sqrt{\pi})^{3.24}(-0.62)}$$

Solving for a_i gives

$$a_i = a_d = 7.63 \times 10^{-5}\text{m} = 0.0763\,\text{mm} \qquad \textbf{Ans.}$$

According to the earlier discussion in Section 11.2.1, this very small a_d is probably below the limits of any reasonable inspection. Hence, periodic inspection would be difficult to avoid in this case unless it is possible to lower the applied load through redesign or restrictions on the use of the component.

Comment It would also be reasonable and more conservative to choose a slightly higher value of F for the N_{if} calculations. For example, choosing $F = 1.03$ gives $N_{if} = 70,500$ cycles for (b) and $a_i = 0.0657$ mm for (d).

11.6.3 Solutions by Numerical Integration

As already discussed, Eq. 11.32 and related equations that might be derived for calculating crack growth life assume that F is constant, so these cannot be used if F changes excessively between the initial and final crack lengths, a_i and a_f. Since closed-form integration of Eq. 11.27 is seldom possible if F is treated as a variable, numerical integration becomes necessary. Also, some elaborate mathematical forms used to fit da/dN versus ΔK curves lead to equations that cannot be integrated in closed form even for constant F, again necessitating numerical integration.

To perform a numerical integration, it is useful to employ Eq. 11.27 in the form of Eq. 11.29. First, pick a number of crack lengths between a_i and a_f:

$$a_i, a_1, a_2, a_3, \ \ldots \ a_f$$

For each of these, and for the material, geometry, and loading of interest, calculate ΔK, and then da/dN, inverting the latter to get dN/da. Finally, find N_{if} as the area under the dN/da versus a curve between a_i and a_f. This can be done for any mathematical form of the ΔK and da/dN equations. For example, for the forms of Eq. 11.30 with F allowed to vary, the dN/da for any given crack length a_j is

$$\left(\frac{dN}{da}\right)_j = \frac{1}{C\left(\Delta K_j\right)^m} = \frac{1}{C\left(F_j \ \Delta S\sqrt{\pi a_j}\right)^m} \tag{11.34}$$

where F_j needs to be specifically calculated for each a_j.

The intervals Δa between the a_j can be made equal, but this is not necessary. It is important that Δa be sufficiently small for accurate representation of the dN/da curve. This is most likely to be a problem for the shorter crack lengths where the curve is generally steepest. One alternative that gives small Δa only where needed is to increase a by a fixed percentage for each interval. A 10% (factor of 1.10) increase for each interval is sufficiently small for typical values of m:

$$a_{j+1} = ra_j, \qquad r \approx 1.10 \tag{11.35}$$

A manual solution for N_{if} may be done on graph paper. It is also straightforward to program an approximate area calculation on a digital computer. Standard methods and computer programs for numerical integration also apply.

A relatively simple method of numerical integration usually described in books on numerical analysis is Simpson's rule. To use this, consider three neighboring crack lengths a_j, a_{j+1}, and a_{j+2}, as shown in Fig. 11.27. Between a_j and a_{j+2}, an estimate of the area under the curve $y = dN/da$ can be made by assuming that a parabola passes through the three points (a_j, y_j), (a_{j+1}, y_{j+1}), and (a_{j+2}, y_{j+2}). If the points are equally spaced Δa apart, the area estimate is

$$\int_{a_j}^{a_{j+2}} y \, da = \frac{\Delta a}{3}\left(y_j + 4y_{j+1} + y_{j+2}\right) \tag{11.36}$$

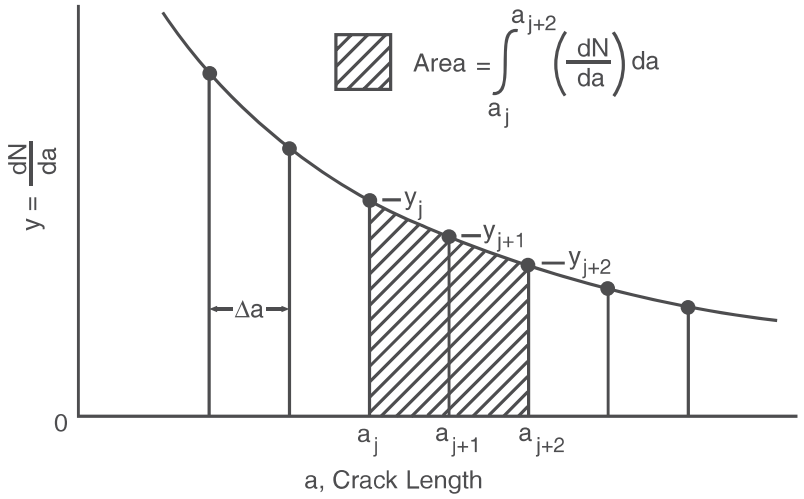

Figure 11.27 Area under the dN/da versus a curve over two intervals Δa as estimated by Simpson's rule.

This equation is applied for each of $j = 0, 2, 4, 6 \ldots (n-2)$, where n is even. Adding the contributions to the area from each calculation gives an approximate value of the total area under the curve between a_i and a_f, where $a_f = a_n$.

For crack growth analysis, the number of intervals can be kept reasonably small if the a values are not evenly spaced, but instead differ by a constant factor r, as in Eq. 11.35. Then

$$a_i, \qquad a_1 = ra_i, \qquad a_2 = r^2 a_i, \qquad \ldots a_n = r^n a_i = a_f \tag{11.37}$$

The area for a parabola through three such points is given by

$$\int_{a_j}^{a_{j+2}} y\, da = \frac{a_j\left(r^2-1\right)}{6r}\left[y_j r(2-r) + y_{j+1}(r+1)^2 + y_{j+2}(2r-1)\right] \tag{11.38}$$

The integration up to a_n can be performed in a manner analogous to a Simpson's rule calculation, except for the use of the new area formula.

Example 11.5

Refine the approximate life estimate of Ex. 11.4(b) by using numerical integration.

Solution The modified Simpson's rule of Eq. 11.38 can be used. A factor for incrementing a is first chosen to be near $r = 1.1$, such that the integration will end at $a_f = 15.8$ mm, which is the a_f as determined in Ex. 11.4. From Eq. 11.37, we have $a_f = r^n a_i$, where $a_i = 1.0$ mm as given. Substituting a_f and a_i with $r = 1.10$ and solving gives $n = 28.96$. Thus, we need an even integer for n near this value. Choosing $n = 30$ and solving for r gives

$$r^n = \frac{a_f}{a_i}, \qquad r^{30} = \frac{15.8\,\text{mm}}{1.0\,\text{mm}}, \qquad r = 1.09637$$

The crack lengths for the $n = 30$ intervals can now be calculated by using this r with Eq. 11.35, starting with the first value as $a_0 = a_i = 0.001$ m. Some of the values are shown in Table E11.5 in units of meters.

Then, using F and S as appropriate for the center-cracked plate geometry from Fig. 8.12(a), we perform calculations as follows for each a_j, where $j = 0$ to 30:

$$\alpha = \frac{a}{b}, \qquad F = \frac{1 - 0.5\alpha + 0.326\alpha^2}{\sqrt{1-\alpha}}$$

$$\Delta K = F\,\Delta S\sqrt{\pi a} = F\,\frac{\Delta P}{2bt}\sqrt{\pi a}, \qquad y = \frac{dN}{da} = \frac{1}{C(\Delta K)^m}$$

Values from Ex. 11.4 are needed as follows: $b = 0.038$ m, $t = 0.006$ m, $\Delta P = 0.160$ MN, $m = 3.24$, and $C = 1.095 \times 10^{-12}$, where this C includes the effect of $R = 0.333$. Note that units of meters, MPa $=$ MN/m^2, and cycles, or combinations of these, are used for all quantities, including C. Some calculation results are shown in Table E11.5.

Next, numerical integration can proceed by applying Eq. 11.38 to each pair of intervals to obtain the number of cycles ΔN to grow the crack from a_j to a_{j+2}:

$$\Delta N_{j+2} = \int_{a_j}^{a_{j+2}} y\,da$$

Specifically, Eq. 11.38 is first applied for the two intervals from $j = 0$ to $j + 2 = 2$, then from $j = 2$ to $j + 2 = 4$, next from $j = 4$ to $j + 2 = 6$, etc., up to $j = 28$ to $j + 2 = 30$. The first

Table E11.5

j	a m	$\alpha = a/b$	$F = F(a/b)$	ΔK MPa$\sqrt{\text{m}}$	$y = dN/da$ cycles/m	ΔN cycles	$\Sigma(\Delta N)$ cycles
0	1.000×10^{-3}	0.0263	1.0003	19.67	5.869×10^{7}	0	0
1	1.096×10^{-3}	0.0289	1.0004	20.60	5.055×10^{7}	—	—
2	1.202×10^{-3}	0.0316	1.0005	21.57	4.354×10^{7}	10 203	10 203
3	1.318×10^{-3}	0.0347	1.0006	22.59	3.750×10^{7}	—	—
4	1.445×10^{-3}	0.0380	1.0007	23.66	3.229×10^{7}	9 098	19 300
5	1.584×10^{-3}	0.0417	1.0008	24.77	2.781×10^{7}	—	—
6	1.737×10^{-3}	0.0457	1.0010	25.94	2.395×10^{7}	8 110	27 410
⋮	⋮	⋮	⋮	⋮	⋮	⋮	⋮
26	1.094×10^{-2}	0.2878	1.0464	68.05	1.052×10^{6}	2 304	72 020
27	1.199×10^{-2}	0.3155	1.0572	71.99	8.770×10^{5}	—	—
28	1.314×10^{-2}	0.3459	1.0708	76.35	7.249×10^{5}	1 935	73 955
29	1.441×10^{-2}	0.3792	1.0881	81.23	5.931×10^{5}	—	—
30	1.580×10^{-2}	0.4158	1.1101	86.78	4.789×10^{5}	1 573	**75 528**

three calculations give

$$\Delta N_2 = \int_{a_0=a_i}^{a_2} y\,da = 10{,}203, \qquad \Delta N_4 = \int_{a_2}^{a_4} y\,da = 9098$$

$$\Delta N_6 = \int_{a_4}^{a_6} y\,da = 8110 \text{ cycles}$$

The cumulative sum of the ΔN values is also calculated as shown in the last column of the table. For example, the number of cycles to reach crack length a_6 is

$$\Sigma(\Delta N)_6 = 10{,}203 + 9098 + 8110 = 27{,}410 \text{ cycles}$$

The final such cumulative sum at $a_{30} = a_f$ is the calculated life for crack growth:

$$\Sigma(\Delta N)_{30} = N_{if} = 75{,}500 \text{ cycles} \qquad \textbf{Ans.}$$

Discussion The life from this numerical integration is seen to be similar to the approximate result from Ex. 11.4 of $N_{if} = 77{,}600$ cycles, which is affected by the choice of $F = 1.00$. If Ex. 11.4 is redone with constant $F = 1.0085$, the same life is obtained as for Ex. 11.5.

11.7 LIFE ESTIMATES FOR VARIABLE AMPLITUDE LOADING

If the stress levels vary during crack growth, life estimates may still be made. One simple approach is to assume that growth for a given cycle is not affected by the prior history—that is, *sequence effects* are absent. Large sequence effects do occur in special situations, but it is often useful and sufficiently accurate to neglect these.

11.7.1 Summation of Crack Increments

The crack growth Δa in each individual cycle of variable amplitude loading can be estimated from the da/dN versus ΔK curve of the material. Summing these Δa, while keeping track of the number of cycles applied, leads to a life estimate. Such a procedure is equivalent to a numerical integration where a, rather than N, is the dependent variable.

Hence, if the current crack length is a_j and the increment is Δa_j, the new value of crack length a_{j+1} for the next cycle is

$$a_{j+1} = a_j + \Delta a_j = a_j + \left(\frac{da}{dN}\right)_j \tag{11.39}$$

where the Δa are numerically equal to da/dN, since $\Delta N = 1$ for one cycle. Denoting the initial crack length as a_i, we find that the crack length after N cycles is

$$a_N = a_i + \sum_{j=1}^{N} \left(\frac{da}{dN} \right)_j \tag{11.40}$$

Each da/dN is calculated from the ΔK and R for that particular cycle, where ΔK is obtained from the current crack length a_j and the ΔS for the particular cycle. Any form of expression for varying $F = F(a/b)$ and any form of a da/dN versus ΔK relationship can be readily used with this procedure. For highly irregular loading, rainflow cycle counting as described in Chapter 9 can be used to identify the cycles.

The summation is continued until a load peak is encountered that is sufficiently severe to cause either fully plastic yielding or brittle fracture. At this point, the calculation is terminated, and the number of cycles accumulated is the estimated crack growth life.

Note that the procedure just described can also be applied for constant amplitude loading as an alternative to the numerical integration approach of Section 11.6.3. In this case, the procedure can be modified to accommodate values of ΔN other than unity, so that cycles are taken in groups, such as $\Delta N = 100$. It is necessary only that ΔN be sufficiently small that da/dN does not change by more than a small amount, so that its value at the beginning of the interval is representative of the entire interval.

For a crack with a curved front, such as a portion of a circle or ellipse, as in Figs. 8.17 to 8.19, the stress intensity K varies around the periphery of the crack. This causes the growth rate to also vary around the periphery, so that the crack changes shape as it grows. This complexity can be handled by updating the crack shape and appropriately adjusting the geometry function F, as crack increments are summed. The needed details for F can be found in various References to Chapter 8, especially Newman (1986). Such a capability is included in the computer programs NASGRO and AFGROW; see LexTech (2010) and SWRI (2010).

11.7.2 Special Method for Repeating or Stationary Histories

In some cases, it may be reasonable to approximate the actual service load history by assuming that it is equivalent to repeated applications of a loading sequence of finite length. This can be useful where some repeated operation occurs, such as lift cycles for a crane, or flights of an aircraft, and also for random loading with characteristics that are constant with time, called *stationary* loading. The crack growth life can then be estimated by an alternative procedure that is equivalent to summing crack increments. The necessary mathematical derivation follows.

First, assume that the da/dN versus ΔK behavior obeys a power relationship of the form of Eq. 11.10. The increment in crack length for any cycle ($\Delta N = 1$) is then

$$\Delta a_j = C_0 \left(\overline{\Delta K}_j \right)^m \tag{11.41}$$

where different R-ratios are handled by calculating an equivalent zero-to-tension ($R = 0$) value $\overline{\Delta K}$, as in the Walker approach using Eq. 11.15. Note that the coefficient C_0 corresponding to $R = 0$ applies due to the use of $\overline{\Delta K}$. If the repeating load history contains N_B cycles, the increase

in crack length during one repetition is obtained by summing:

$$\Delta a_B = \sum_{j=1}^{N_B} \Delta a_j = \sum_{j=1}^{N_B} C_0 \left(\overline{\Delta K}_j\right)^m \tag{11.42}$$

The average growth rate per cycle during one repetition of the history is thus

$$\left(\frac{da}{dN}\right)_{\text{avg.}} = \frac{\Delta a_B}{N_B} = \frac{C_0 \sum_{j=1}^{N_B} \left(\overline{\Delta K}_j\right)^m}{N_B} \tag{11.43}$$

Note that C_0 is constant and so can be factored from the summation. Manipulation gives

$$\left(\frac{da}{dN}\right)_{\text{avg.}} = C_0 \left(\left[\frac{\sum_{j=1}^{N_B} \left(\overline{\Delta K}_j\right)^m}{N_B} \right]^{1/m} \right)^m = C_0 \left(\Delta K_q\right)^m \tag{11.44}$$

where

$$\Delta K_q = \left[\frac{\sum_{j=1}^{N_B} \left(\overline{\Delta K}_j\right)^m}{N_B} \right]^{1/m} \tag{11.45}$$

The quantity ΔK_q can be interpreted as an equivalent zero-to-tension stress intensity range that is expected to cause the same crack growth as the variable amplitude history when applied for the same number of cycles N_B.

Since K and nominal stress S are proportional for any given crack length, an equivalent zero-to-tension stress level can also be defined:

$$\Delta S_q = \frac{\Delta K_q}{F\sqrt{\pi a}} = \left[\frac{\sum_{j=1}^{N_B} \left(\overline{\Delta S}_j\right)^m}{N_B} \right]^{1/m} \tag{11.46}$$

In this equation, the $\overline{\Delta S}$ for each cycle in the history is the equivalent zero-to-tension value corrected for R effect. If this is done on the basis of the Walker approach using Eq. 11.15, these values are obtained from

$$\overline{\Delta S} = S_{\max}(1 - R)^{\gamma} \tag{11.47}$$

where γ is the value for crack growth, as from Table 11.2.

Since ΔS_q is independent of crack length, it can be applied throughout the life as the crack grows. Hence, we can make a life estimate by using ΔS_q just as if it were a constant amplitude loading at $R = 0$, for example, by using Eq. 11.32. However, to determine the final crack length a_f as caused by either fully plastic yielding or brittle fracture, the actual peak stress $S_{\max}$ in one repetition of the history should be employed.

Such use of ΔS_q assumes that the load history of length N_B is repeated numerous times during the crack growth life. If the repeating history is so long that only a few repetitions occur, then special, detailed handling of the last repetition is needed to identify the load peak that causes failure and so determines a_f.

Note that Eq. 11.46 is very similar to Eq. 9.37, which is employed for calculating equivalent stress amplitudes for use with stress–life curves. If the latter is expressed in terms of stress range and equivalent zero-to-maximum stresses, the two become identical with the substitution $m = -1/b$.

Example 11.6

A center-cracked plate of the AISI 4340 steel of Table 11.2 has dimensions, as defined in Fig. 8.12(a), of $b = 38$ and $t = 6$ mm, and the initial crack length is $a_i = 1$ mm. It is repeatedly subjected to the axial force history of Fig. E11.6. How many repetitions of this history can be applied before fatigue failure is expected? (This is the same situation as Ex. 11.4, except for the load history.)

Solution We will first calculate an equivalent zero-to-tension stress level for the load history from Eq. 11.46. This ΔS_q may then be employed in Eq. 11.32 to calculate the life N_{if} as if it were a simple zero-to-tension ($R = 0$) loading. However, a_f needs to correspond not to ΔS_q, but to the most severe force in the history, $P_{\max} = 240$ kN. Since this $P_{\max}$ is the same as in Ex. 11.4, we need not repeat the calculation, but may employ the a_f value and corresponding approximate F from Ex. 11.4, which are

$$a_f = 15.8 \text{ mm}, \qquad F = 1.00$$

In addition, materials properties from Table 11.2 are needed:

$$C_0 = 5.11 \times 10^{-13} \frac{\text{m/cycle}}{(\text{MPa}\sqrt{\text{m}})^m}, \qquad m = 3.24, \qquad \gamma = 0.42$$

From rainflow counting of the given force history, we obtain the results presented in the first four columns of Table E11.6. The single cycle for $j = 4$ arises from rainflow cycle counting as the major cycle between the highest peak and lowest valley. (See Section 9.9.2).

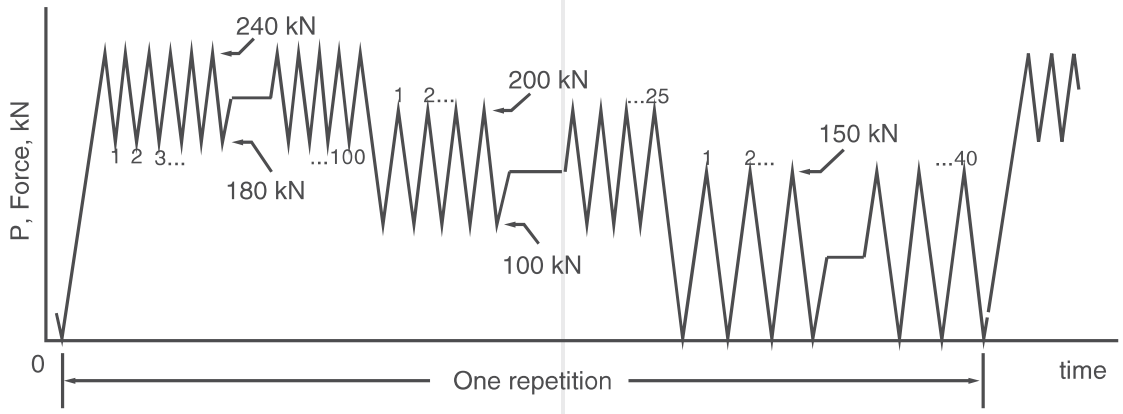

Figure E11.6

Table E11.6

j	N_j cycles	$P_{\max}$ kN	$P_{\min}$ kN	R	$S_{\max}$ MPa	$\overline{\Delta S}_j$ MPa	$N_j(\overline{\Delta S}_j)^m$
1	100	240	180	0.75	526.3	294.0	9.94×10^9
2	25	200	100	0.5	438.6	327.8	3.54×10^9
3	40	150	0	0	328.9	328.9	5.72×10^9
4	1	240	0	0	526.3	526.3	6.56×10^8
Σ	166						1.986×10^{10}

The following calculations are then needed for each load level j:

$$R = \frac{P_{\min}}{P_{\max}}, \qquad S_{\max} = \frac{P_{\max}}{2bt}, \qquad \overline{\Delta S} = S_{\max}(1 - R)^{\gamma}$$

Here, S is defined as in Fig. 8.12(a).

Since multiple cycles occur at each of $k = 4$ load levels, the summation for Eq. 11.46 may be done in the form

$$\sum_{j=1}^{N_B} (\overline{\Delta S}_j)^m = \sum_{j=1}^{k} N_j (\overline{\Delta S}_j)^m$$

Details are given in Table E11.6, where the sum is shown at the bottom. Noting that $N_B = \Sigma N_j = 166$ cycles, we may now calculate ΔS_q:

$$\Delta S_q = \left[\frac{\sum_{j=1}^{k} N_j (\overline{\Delta S}_j)^m}{N_B} \right]^{1/m} = \left[\frac{1.986 \times 10^{10}}{166} \right]^{1/3.24} = 311.3 \text{ MPa}$$

This value is then employed in Eq. 11.32 to obtain the number of cycles for crack growth:

$$N_{if} = \frac{a_f^{1-m/2} - a_i^{1-m/2}}{C_0 (F\, \Delta S_q \sqrt{\pi})^m (1 - m/2)} = \frac{0.0158^{-0.62} - 0.001^{-0.62}}{5.11 \times 10^{-13} (1.00 \times 311.3 \sqrt{\pi})^{3.24} (-0.62)}$$

$$N_{if} = 2.45 \times 10^5 \text{ cycles}$$

Here, all quantities substituted correspond to units of meters and MPa, as in Ex. 11.4. Also, C_0 is the value for $R = 0$, as R-ratio effects are already included in the $\overline{\Delta S}$ values. Finally, the number of repetitions to failure is

$$B_{if} = \frac{N_{if}}{N_B} = \frac{2.45 \times 10^5}{166} = 1477 \text{ repetitions} \qquad \textbf{Ans.}$$

11.7.3 Sequence Effects

In all of the treatment so far of variable amplitude loading, it has been assumed that the crack growth in a given cycle is unaffected by prior events in the load history. However, this assumption may sometimes lead to significant error. Consider the situation of Fig. 11.28. After a high tensile overload is applied, as in case C, the growth rate during the lower level cycles is decreased. Slower than normal growth continues for a large number of cycles until the crack grows beyond the region affected by the overload, where the size of the affected region is related to the size of the crack-tip plastic zone caused by the overload. For the case illustrated, the overall effect of only three overloads was to increase the life by about a factor of 10. This beneficial effect of tensile overloads is called *crack growth retardation*.

A tensile overload introduces a compressive residual stress around the crack tip in a manner similar to the notched member of Fig. 10.28. This compression tends to keep the crack tip closed during the subsequent lower level cycles, retarding crack growth. The magnitude of the effect is related to the ratio $S_{\max 2}/S_{\max 1}$, where $S_{\max 2}$ is the overload stress and $S_{\max 1}$ is the peak value of the lower level. For ratios greater than about 2.0, crack growth may be *arrested*—that is, stopped entirely. Conversely, if the ratio is less than about 1.4, the effect is small. Compressive overloads have an opposite, but lesser, effect. The effect is not as great because the crack tends to close during the overload, so the faces of the crack support much of the compressive load and shield the crack tip from its effect. Also, the effect of a tensile overload is much reduced if it is followed by a compressive one, as in case B of Fig. 11.28.

Several methods have been developed to incorporate sequence effects due to overloads into life calculations for crack growth. The general approach used is to base the life estimate on calculating crack growth increments for each cycle as previously described in connection with Eqs. 11.39 and 11.40. However, the da/dN values used are modified in a manner that is determined by the prior history of overloads. This is generally done by determining da/dN from an effective

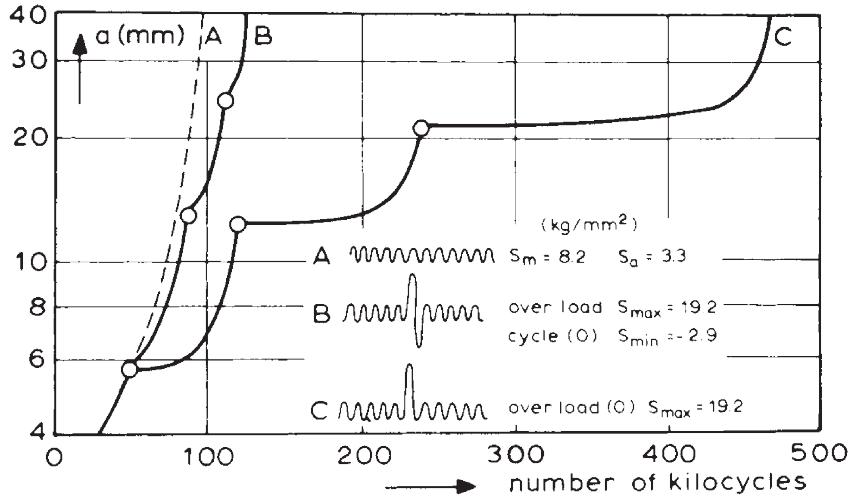

Figure 11.28 Effect of overloads on crack growth in center-cracked plates ($b = 80$, $t = 2$ mm) of 2024-T3 aluminum. (From [Broek 86] p. 273, based on data in [Schijve 62]; reprinted by permission of Kluwer Academic Publishers.)

ΔK that is modified on the basis of logic related to residual stress fields or crack closure levels. More detailed explanation can be found in Broek (1986) and (1988), Grandt (2004), and Suresh (1998).

Overload sequence effects are likely to be important where high overloads occur predominantly in one direction. This occurs in the service of some aircraft, where occasional severe wind gust loadings or maneuver loadings may introduce sequence effects. However, less effect is expected if overloads occur in both directions, if the history is highly irregular, or if the overloads are relatively mild. Noting that the effect is mainly to retard crack growth, we see that neglecting this sequence effect usually provides conservative estimates of crack growth life that will be sufficient for engineering purposes in many cases. Load histories that include severe compressive overloads then need to be handled with caution, due to the possibility of these causing faster crack growth than predicted.

11.8 DESIGN CONSIDERATIONS

It is becoming increasingly common to ensure adequate service life for components of machines, vehicles, and structures on the basis of crack growth calculations, as described in this chapter. This is appropriate for large structures subjected to cyclic loading, especially where personal safety or high costs are factors, and especially if cracks are commonly found in the type of hardware involved. Examples include bridge structure, large aircraft, space vehicles, and nuclear and other pressure vessels. Such a *damage-tolerant* approach is critically dependent on initial and sometimes periodic inspections for cracks.

Inspection for cracks, especially small ones, is an expensive process and is not generally feasible for inexpensive components that are made in large numbers. If the service stresses are relatively high, the cracks that would need to be found to use a damage-tolerant approach can be so small that the inspection would greatly increase the cost of the item. Periodic inspections would allow a larger crack to be tolerated initially, but the component may not be available for periodic inspection. Examples of parts that fall into this category are automobile engine, steering, and suspension parts, bicycle front forks and pedal cranks, and parts for home appliances. Here, fatigue life estimates are usually made on the basis of an *S*-*N* approach, or the related strain-based approach, neither of which specifically considers cracks. Where personal safety is involved, safety factors reflect this fact and are typically larger than if a damage-tolerant approach could be used. Failures are minimized by careful attention to design detail and to manufacturing quality control, including initial inspection to eliminate any obviously flawed parts.

Regardless of the approach used, a finite probability of failure always exists. For the damage-tolerant approach, this arises because the minimum detectable crack length a_d is difficult to establish and is never precisely known. For the *S*-*N* and related approaches, a finite probability of failure arises due to the possibility that a part passing inspection still contains a flaw that, though small, nevertheless leads to early failure. Also, all approaches to ensuring adequate life are subject to additional uncertainties, such as: (1) estimates of the service loading being too low, (2) accidental substitution during manufacturing of the wrong material, (3) undetected manufacturing quality control problems, and (4) hostile environmental effects that are more severe than forecast, with the latter including both ordinary corrosion and environmental crack growth.

Where a damage-tolerant approach is used, critical components must be designed so that they are accessible for inspection. For example, cracks at fastener (rivet or bolt) holes are of concern in aircraft structure, and access to the interior of the skin of the fuselage or wing structure may be needed for situations such as that illustrated in Fig. 11.29. If periodic inspections are required, then the design must accommodate disassembly when this is necessary for inspection. For example, in large aircraft, the passenger seats, interior panels, and even paint are removed, and some structural parts are disassembled, for costly, but necessary, periodic inspections.

Specific measures can also be taken by the designer to allow structures to function without sudden failure even if a large crack does develop. Some examples for aircraft structure are illustrated in Figs. 11.30 and 11.31. Stiffeners retard crack growth, and joints in skin panels may be

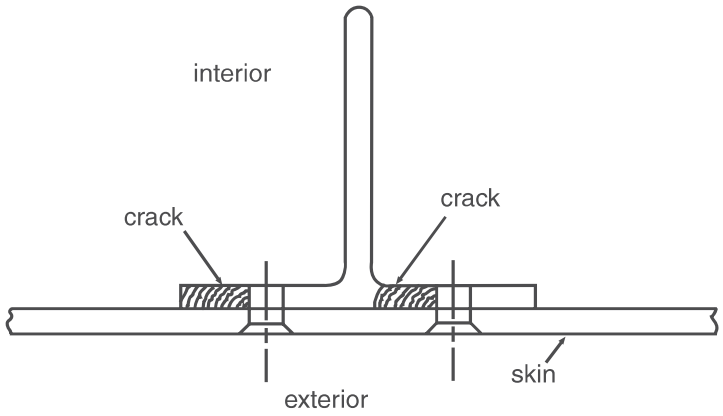

Figure 11.29 Cracks in the interior of an aircraft skin structure. (Adapted from [Chang 78].)

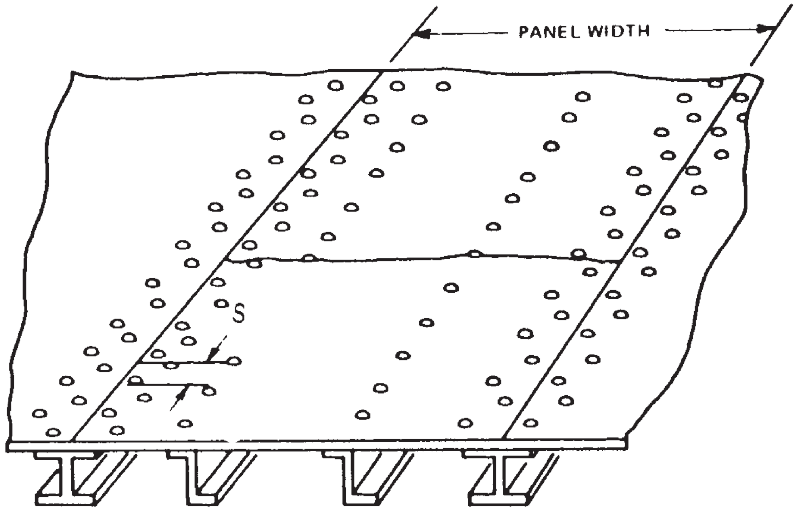

Figure 11.30 Stiffened panel in aircraft structure with a crack delayed before growing into adjacent panels. The rivet spacing dimensioned is 38 mm. (From the paper by J. P. Butler in [Wood 70] p. 41.)

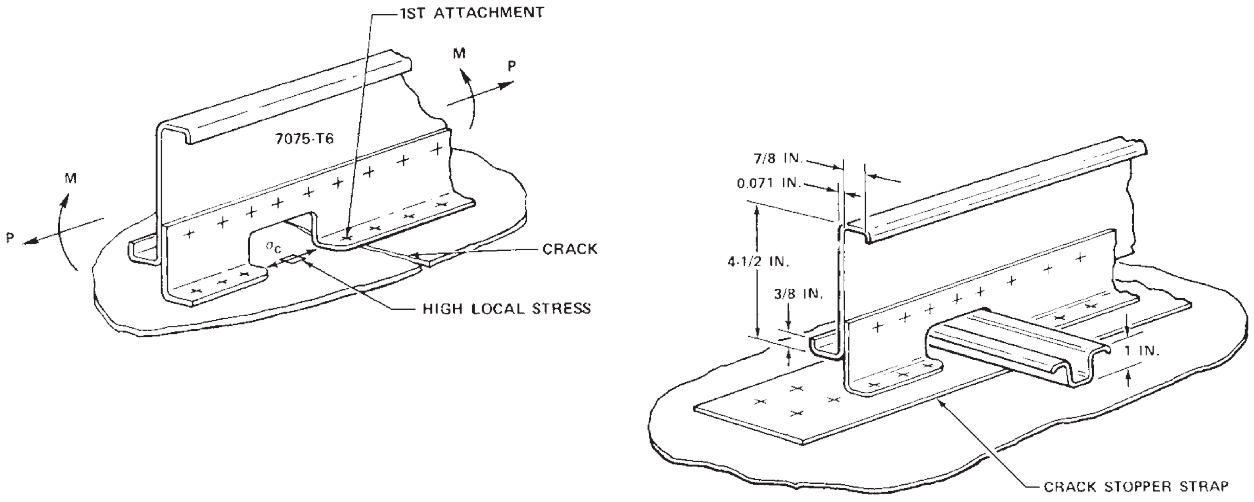

Figure 11.31 Crack (left) in a DC-10 fuselage in the longitudinal direction, due to cabin pressure loading, and (right) a crack stopper strap. Rivet locations are indicated by (+), and the longeron member with a hat-shaped cross section is omitted on the left for clarity. (From [Swift 71]; copyright © ASTM; reprinted with permission.)

intentionally introduced so that a crack in one panel has difficulty growing into the next. Similarly, a crack stopper strap may lower stresses in a critical area and provide some strength even if a crack does start.

Recall from the early part of this chapter and Eq. 11.2 that the safety factor on life X_N is the ratio of the failure life for crack growth N_{if} to the expected service life $\hat{N}$. The value of N_{if} depends not only on the detectable crack length a_d, but also on the stress level and the material. If the safety factor is insufficient, perhaps even less than unity, several different options exist to resolve the situation. Obviously, the design could be changed to lower the stress, thus increasing the calculated life N_{if} and X_N. Another possibility is to make a more careful initial inspection for cracks, decreasing a_d, and thus increasing the worst-case failure life N_{if}. Alternatively, the material could be changed to one with slower fatigue crack growth rates, as judged by comparing da/dN versus ΔK curves. Depending on whether failure occurs by brittle fracture or by yielding, increasing either the fracture toughness or the yield strength of the material also increases the life by increasing the final crack length a_f, but the effect is usually small, as the life is generally insensitive to the value of a_f.

If design changes or improved initial inspection do not suffice, it may be necessary to perform periodic inspections, making it permissible to calculate the safety factor from the inspection period N_p with the use of Eq. 11.5.

11.9 PLASTICITY ASPECTS AND LIMITATIONS OF LEFM FOR FATIGUE CRACK GROWTH

During cyclic loading, a region of reversed yielding exists at the crack tip, and the size of this region can be estimated by a procedure similar to that applied to static loading in Section 8.7. On this

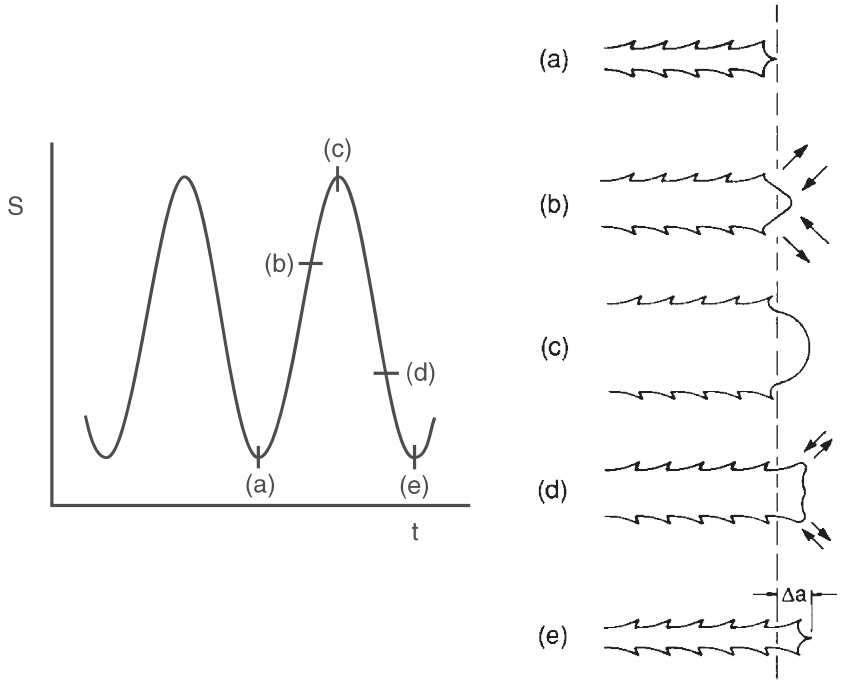

Figure 11.32 Hypothesized plastic deformation behavior at the tip of a growing fatigue crack during a loading cycle. Slip of crystal planes along directions of maximum shear occurs as indicated by arrows, and this plastic blunting process results in one striation (Δa) being formed for each cycle. (Adapted from the paper by J. C. Grosskreutz in [Wood 70] p. 55.)

basis, plasticity limitations on LEFM for fatigue crack growth can be explored. Limitations are also needed if the crack is so small that its size is comparable to that of the microstructural features of the material.

11.9.1 Plasticity at Crack Tips

In the immediate vicinity of the crack tip, there is a finite separation δ between the crack faces, as discussed in Chapter 8. Behavior on the size scale of δ determines how the crack advances through the material during cyclic loading. Details are not fully understood, they vary with material, and they even vary with the K level for a given material. In ductile metals, the process of crack advance during a cycle is thought to be similar to Fig. 11.32. Localized deformation by slip of crystal planes occurs and is most intense in bands above and below the crack plane. The crack tip moves ahead and becomes blunt as the maximum load is reached, and it is resharpened during decreasing load. This process results in striations on the fracture surface, as previously illustrated by Fig. 9.22.

Another mechanism is crack growth by small increments of brittle cleavage during each cycle. It is not uncommon in metals for the fracture surface to have regions of striation growth mixed with regions of cleavage, especially at high growth rates where $K_{\max}$ approaches K_c. In other cases, the boundaries between grains are the weakest regions in the material, so that the crack grows along grain boundaries. This is called *intergranular fracture*, to distinguish it from the more

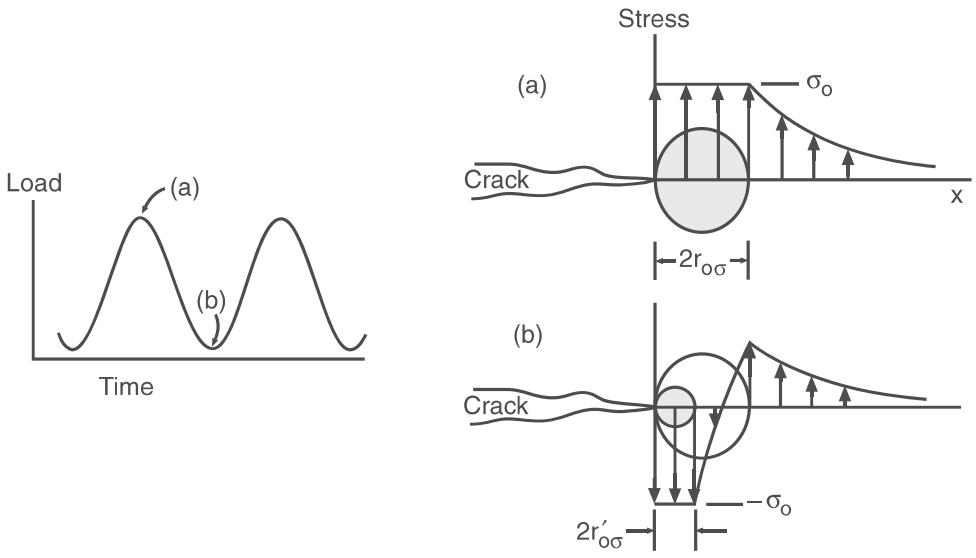

Figure 11.33 Monotonic (a) and cyclic (b) plastic zones. (Adapted from [Paris 64]; used with permission.)

usual *transgranular fracture* by striation formation or cleavage. For example, intergranular fatigue cracking occurred for the granite rock of Fig. 11.11. In metals, intergranular cracking is likely to occur if there is a hostile environmental influence.

If the material is relatively ductile, a crack-tip plastic zone will exist that is considerably larger than δ. The peak stress in the cyclic loading determines $K_{\max}$, which can be substituted into Eq. 8.37 or 8.38 to estimate the extent of yielding ahead of the crack. For example, for plane stress,

$$2r_{o\sigma} = \frac{1}{\pi}\left(\frac{K_{\max}}{\sigma_o}\right)^2 \tag{11.48}$$

This is called the *monotonic plastic zone*. As the minimum load in a cycle is approached, yielding in compression occurs in a region of smaller size, called the *cyclic plastic zone*, as illustrated in Fig. 11.33.

For an ideal elastic, perfectly plastic material, consider the behavior during unloading following $K = K_{\max}$. For compressive yielding to occur as K changes by an amount ΔK, the stress of σ_o near the crack tip must change to $-\sigma_o$, which is a change of $2\sigma_o$, or twice the yield strength. In effect, for changes relative to $K_{\max}$, the yield strength is doubled. The size of the cyclic plastic zone where yielding occurs not only in tension, but also in compression, can therefore be approximated by using ΔK for K and $2\sigma_o$ for σ_o in the monotonic plastic zone estimate:

$$2r'_{o\sigma} = \frac{1}{\pi}\left(\frac{\Delta K}{2\sigma_o}\right)^2 \tag{11.49}$$

For zero-to-tension ($R = 0$) loading, where $\Delta K = K_{\max}$, the cyclic plastic zone is thus estimated to be one-fourth as large as the monotonic one. The cyclic plastic zone size may also be estimated

for cases of plane strain. Using logic as in Section 8.7, we see that its size $r'_{o\varepsilon}$ is one-third as large as the corresponding plane stress zone.

We can further understand the monotonic and cyclic plastic zones by considering the stress–strain history at a point in the material as the crack approaches, as illustrated in Fig. 11.34. When the point being observed is still outside the monotonic plastic zone, no yielding occurs. Yielding begins, but only in the tensile direction, when the monotonic plastic zone boundary passes the point. Once the cyclic plastic zone boundary passes, yielding in both compression and tension occurs during each loading cycle.

11.9.2 Thickness Effects and Plasticity Limitations

If the monotonic plastic zone is not small compared with the thickness, then plane stress exists, and fatigue cracks may grow in a shear mode, with the fracture inclined about 45° to the surface. Since K and hence the plastic zone size increase with crack length, a transition to this behavior can occur during the growth of a crack, as illustrated in Fig. 11.35. Crack growth rates can be affected somewhat by member thickness as a result of different behavior in plane stress and plane strain. However, the effect is sufficiently small that it can generally be ignored, so crack growth data for one thickness can be used for any other thickness.

If large amounts of plasticity occur during cyclic loading, crack growth rates rapidly increase and exceed what would be expected from the da/dN versus ΔK curve. This circumstance arises from the fact that the theory supporting the use of K requires that the plasticity be limited to a

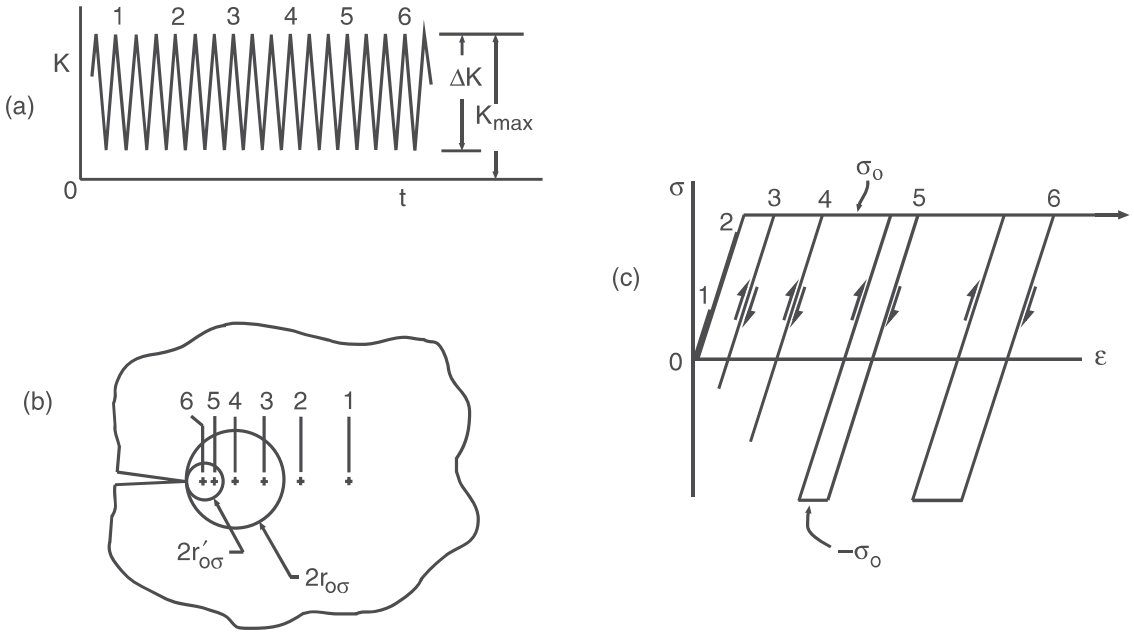

Figure 11.34 Stress–strain behavior at a point as the tip of a growing fatigue crack approaches. For selected cycles (a), relative positions of the point and the crack tip are shown in (b), and the stress–strain responses in (c). (Adapted from [Dowling 77]; copyright © ASTM; reprinted with permission.)

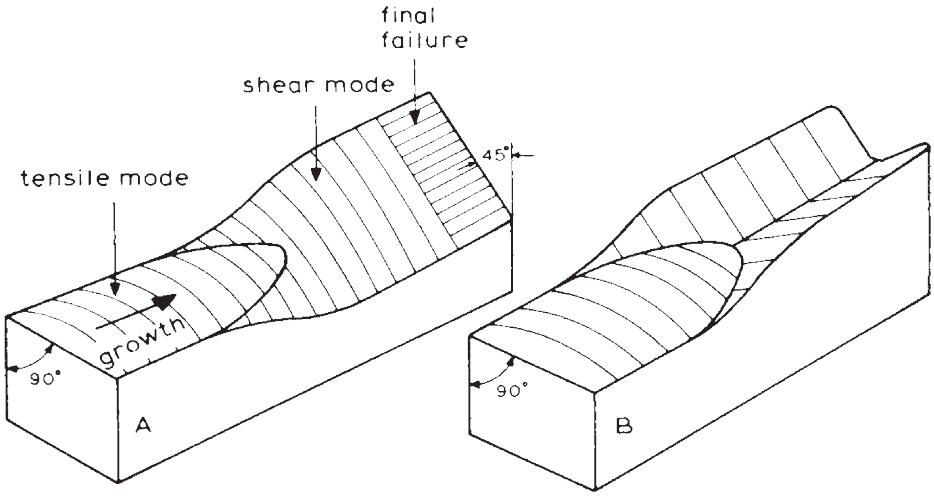

Figure 11.35 Schematic of surfaces of fatigue cracks showing transition from a flat tensile mode to an angular shear mode. The shear growth can (A) occur on a single sloping surface, or (B) form a *V*-shape. (From [Broek 86] p. 269; reprinted by permission of Kluwer Academic Publishers.)

region that is small compared with the planar dimensions of the member, as discussed previously in Section 8.7. Large effects occur only where the maximum load exceeds about 80% of fully plastic yielding, so this level represents a sufficient plasticity limitation in most cases. Modest effects may occur at somewhat lower levels. If a fairly strict limitation is desired, the limitation of Eq. 8.39 on the in-plane dimensions, as previously employed for static loading, can be applied to the peak stress:

$$a, (b-a), h \geq 8r_{o\sigma} = \frac{4}{\pi}\left(\frac{K_{\max}}{\sigma_o}\right)^2 \tag{11.50}$$

For fatigue crack growth, thickness effects and plasticity limitations are not generally issues of major importance, as they are for fracture toughness applications. This is because nominal stresses around or exceeding yielding are rare in engineering situations except near the very end of the life, when the fatigue crack growth phase is essentially complete. However, local yielding at stress raisers is fairly common, so difficulties may be encountered if it is necessary to use fracture mechanics for cracks growing from notches while they are still small, as they may be affected by local plasticity. Fortunately, a crack is under the influence of the local stress field of a notch only if its length is quite small, specifically less than about 10 to 20% of the notch radius. See Eq. 8.26 and Fig. 8.20.

11.9.3 Limitations for Small Cracks

Fracture mechanics in the form considered so far is based on stress analysis in an isotropic and homogeneous solid. The microstructural features of the material are, in effect, assumed to occur on such a small scale that only the average behavior needs to be considered. However, if a crack is sufficiently small, it can interact with the microstructure in ways that cause the behavior to differ from what would otherwise be expected. In engineering metals, small cracks tend to grow faster